SUPPLEMENTARY MATERIAL

Supplementary methods

Energy intake and feces lipid content

The amount of food consumed was monitored from each cage and converted to daily intake per mouse. Average daily energy intake was calculated by converting the amount of food consumed into joules using the information provided by the diet manufacturer (LabDiet, TestDiet, USA). Lipid extraction for feces lipid content analysis was performed based on established procedures.[1]

Cecal and colonic short-chain fatty acids

Short-chain fatty acids (SCFAs), including acetate, propionate and butyrate, were measured in cecal and colonic samples using gas chromatography (6890N, Agilent Technologies, USA).[2] Supernatants (2 ml) were prepared by reconstituting all cecal content of each animal in 0.01 M of PBS, followed by centrifugation at 9,000g for 5 min at 4°C. Supernatants were acidified with nine volumes of 50% H_2SO_4 and extracted with ethyl ether. SCFA concentrations were measured in the organic phase using a gas chromatograph equipped with a polar HP-FFAP capillary column (0.25 mm × 0.25 mm × 30 m) and a flame ionization detector (Agilent Technologies). Helium was used as the carrier gas. Oven temperature was set at 140°C. Temperature was maintained for 10 min, raised to 165°C at 5°C/min, increased to 270°C at 25°C/min, and held at this temperature for 2 min. Detector temperature was set at 280°C and the injector temperature was 250°C. SCFAs were quantified by comparing peak areas with those of chemical standards. Data were obtained with the Agilent ChemStation (version G2070AA, Agilent Technologies).

Histopathological staining and scoring

Visceral adipose tissues (VATs), brown adipose tissues (BATs) and inguinal white adipose tissues (iWATs) were dissected and weighed following animal sacrifice. Subsections were partially embedded in 10% neutral buffered formalin (NBF) solution (Sigma, USA). The hepatic central lobe was collected and punched sections were fixed in 10% NBF. Paraffin-embedded hepatic central lobe and adipose tissue sections (4 μm) were stained with hematoxylin and eosin (H&E) for morphological examination. Slides were scanned with the NanoZoomer 2.0-HT slide scanner (Hamamatsu, Germany) and scanned sections were captured using Aperio

ImageScope (Leica Biosystems Imaging, USA). Quantification of adipocyte size was performed from five microscopy fields for each mouse using the Adiposoft software (Image J). The number of crown-like structures (CLS) consisting of dead adipocytes surrounded by macrophages was quantified. Scoring of non-alcoholic steatohepatitis activity index (NAI) was done based on five parameters described in a previous study,[3] including microvesicular steatosis, macrovesicular steatosis, hepatocellular hypertrophy, inflammation and fibrosis (supplementary dataset S1).

Immunohistochemistry staining

Immunohistochemistry staining (IHC) was performed on 4 μm paraffin-embedded sections using the Benchmark XT slide staining system combined with the OptiView DAB IHC Detection Kit (Ventana Medical Systems, USA) according to the manufacturer's protocol. Sections were hybridized with rabbit-anti-mouse uncoupling protein 1 antibody (UCP1, dilution 1:70, Proteintech, USA), exposed to 3,3-diaminobenzidine (DAB). Cell nuclei were counterstained with hematoxylin. Slides were scanned and observed as above.

Serum biochemical analysis

Biochemical analysis of serum samples was performed using an automatic Hitachi 7080 Chemistry Analyzer (Hitachi, Japan) based on the information provided by the manufacturer.

Oral glucose tolerance test and insulin tolerance test

For the oral glucose tolerance test (OGTT), 8-hr-fasted mice were treated with a glucose solution (10%, w/v) by intragastric gavage (1 g/kg). For the insulin tolerance test (ITT), 6-hr-fasted mice were injected intraperitoneally with insulin (0.5 IU/kg). Blood glucose levels were measured from tail vein blood using a glucometer (OneTouch Glucose Meters, USA). Total area under the curve (AUC) was calculated using the trapezoidal method.[4]

RNA extraction and quantitative real-time PCR analysis

Total RNA was extracted from proximal colon tissues using the Tri Reagent Kit (Sigma, USA) according to the manufacturer's instructions. Equal amounts of RNA were used to synthesize cDNA using the Quant II fast RT kit (Tools, Taiwan). cDNA was used for quantitative real-time PCR (qRT-PCR) with the KAPA SYBR FAST

Universal 2× qPCR Master Mix (Kapa Biosystems, USA). Expression of IL-1β, TNF-α, ZO-1 and the housekeeping gene glyceraldehyde-3-phosphate dehydrogenase (GAPDH) was assessed by qRT-PCR. Relative amount of transcripts for target genes was determined for each cDNA sample after normalization against GAPDH or 18S rRNA. Data were analyzed using the $2^{-\Delta\Delta CT}$ method.[5] Primer sequences for qRT-PCR are shown in supplementary table S4.

Flow cytometry analysis

Isolation of mononuclear cells in mouse colonic lamina propria was performed as described previously.[6] Flow cytometry analysis was performed using a FACSCalibur flow cytometer (BD, USA). Data were analyzed using the FlowJo software (v.9.3.2, FlowJo, USA). IL-1β-expressing M1 macrophages were first gated with the F4/80 positive population and identified as CD11c and IL-1β double-positive cells. IL-10-expressing regulatory T cells were first gated with the CD4 positive population and identified as Foxp3 and IL-10 double-positive cells.

Fecal microbiota transplantation

Chow- and HFD-fed donor mice (5-week old, male) were treated daily with saline, HSM, H1 and H4 via oral gavage for 4 weeks, followed by daily collection of feces. Feces pellets (80–110 mg) from each donor mice were collected daily in autoclaved tubes and homogenized in 1 ml of sterile saline. Homogenized fecal mixtures were centrifuged for 1 min at 2,000g at 4°C. Supernatants were transferred to new tubes and centrifuged for 5 min at 15,000g to precipitate bacteria. Bacterial pellets were resuspended in 600 μl of sterile saline. HFD-fed mice (5-week old, male) were inoculated daily with 100 μl of fecal microbiota transplants from each donor group via oral gavage for 12 weeks (supplementary figures 10–12). The FMT procedure from collection of fecal microbiota to oral gavage was completed within 1 hr.

Cecal microbiota DNA extraction

Cecal microbiota DNA was extracted using the QIAamp DNA Stool Mini Kit (Qiagen, USA). Cecal content (in vivo antibiotics treatment and recipients of ex FMT) and fecal pellets (donors of ex FMT) were added to a tube containing a sterilized steel bead, prior to treatment as described in the manufacturer's instructions. Tubes containing specimen and steel bead were placed into a benchtop homogenizer (TissueLyser II, Qiagen) and disrupted for 30 seconds three times, with a 1-min rest

period. Microbiota samples were collected by low-speed centrifugation and high-speed centrifugation after homogenization, and further treated as described in the manufacturer's instructions. DNA concentration was measured using the NanoPhotometer P360 (Implen, USA).

Illumina HiSeq sequencing and library construction

Cecal or fecal samples were snap-frozen in liquid nitrogen and stored at –80°C. DNA was extracted using a fecal DNA isolation kit (Qiagen). 16S rRNA gene comprising the V3–V4 regions was amplified using composite primers containing a unique 10-base barcode to tag PCR products. PCR mix (50 µl) contained 25 ng DNA template, 5× HiFi buffer, 10 mM dNTP mix, 1 unit/µl HiFi DNA polymerase (KAPA Biosystems, USA) and 0.3 µM of composite primer pairs. PCR reaction conditions consisted of denaturation at 95°C for 3 min, followed by 15–25 cycles of 98°C for 20 sec, 45°C for 15 sec, and 72°C for 15 sec, and a final extension of 72°C for 1 min. Composite primers consisted of the forward primer 5'-TCGTCGGCAGCGTCAGATGTGTATAAGAGACAG*CCTAYGGGRBGCASCAG*-3', which contains the Illumina forward overhang adaptor sequence (underlined) and the universal bacterial primer 341F (italicized), and the reverse primer 5'-GTCTCGTGGGCTCGGAGATGTGTATAAGAGACAG*GGACTACNNGGGTATCTAAT*-3', which contains the Illumina reverse overhang adaptor sequence (underlined) and the broad-range bacterial primer 806R (italicized). Replicate PCRs were pooled and amplicons were purified using the QiaQuick PCR Purification Kit (Qiagen). PCR amplicons were sequenced using the Illumina sequencing platform following the instructions of the manufacturer and HiSeq procedures. Sequencing libraries were generated using the TruSeq DNA PCR-Free Sample Preparation Kit (Illumina, USA) following the manufacturer's recommendations. Library quality was assessed using the Qubit@ 2.0 Fluorometer (Thermo Scientific) and Agilent Bioanalyzer 2100 system. The library was sequenced on an Illumina HiSeq 2500 platform and 250 bp paired-end reads were generated. Sequence datasets were deposited into the Sequence Read Archive (accession numbers SRP139890 and SRP139903).

16S rDNA-based metagenomics analysis

Amplicon sequencing was performed using 250 bp paired-end raw reads and the entire paired-end reads were assembled using FLASH v.1.2.7.[7] Low-quality reads (Q score <20) were discarded in QIIME 1.7.[8] If three consecutive bases were <Q20, the

read was truncated and the resulting read was retained in the data only if it was at least 75% of the original length[9] (QIIME script split_libraries_fastq.py). Sequences were chimera-checked using UCHIME[10, 11] and filtered from the data set before operational taxonomic unit (OTU) picking of 97% sequence identity using USEARCH v.7 pipeline[12] (UPARSE function).[13] For each representative sequence, the Greengenes Database version 13_8[14, 15] was used based on RDP classifier (v.2.2) algorithm[16] to annotate taxonomy classification. Any sequences presented once (singletons) or in only one sample were filtered out. In order to identify the relationship between different OTUs, multiple sequence alignment was conducted using the PyNAST software (v.1.2)[17] against the core-set dataset in the Greengenes database. A phylogenetic tree was constructed with a set of sequences representative of the OTUs using the FastTree,[18, 19] which was already included in QIIME. To avoid sampling depth bias, OTUs abundance information was rarefied to the minimum sequences across samples by random sampling (without replacement) of the raw OTU abundance (QIIME script single_rarefaction.py). Beta diversity analysis was used to evaluate differences of samples in species complexity. Beta diversity on weighted UniFrac[20, 21] was calculated using the QIIME software. Principal coordinate analysis (PCoA) was performed to obtain principal coordinates and visualize complex, multidimensional data. PCoA analysis was displayed using the WGCNA package, stat packages and ggplot2 package of the R software (v.2.15.3). To analyse significant differences between groups, permutational multivariate analysis of variance (PERMANOVA) tests (9,999 permutations) were performed on the weighed UniFrac distance matrices using QIIME. Unweighted pair-group method with arithmetic means (UPGMA) clustering was performed as a type of hierarchical clustering method to interpret the distance matrix using average linkage using the QIIME software. For comparing metagenomic samples, significance of all species between groups on various taxonomic levels were tested using Metastats.[22] The *P* values of comparison between two groups were calculated using an equation suggested in the Metastats software, when less than 8 subjects were used in each treatment. OTUs were searched against the GenBank sequence database (National Center for Biotechnology Information, NCBI, USA; assignment was based on >97% identity and 100% coverage of 16S rRNA genes). Heatmaps were drawn using MeV version 4.8.1.

Quantification of fecal and cecal microbiota by quantitative PCR

Levels of *P. goldsteinii* in fecal and cecal microbiota were determined using real-time

quantitative PCR (7900HT, Applied Biosystems, USA) and specific primers (supplementary table S4), along with the KAPA SYBR FAST master mix (2×) qPCR kit (Kapa Biosystems, USA). Standard curves were determined from the CT values of serial diluted plasmid (pHE vector, Biotools, Taiwan) containing single copy of full-length of *P. goldsteinii* which is amplified using 16S rDNA V1–V9 primers (supplementary table S4). The absolute copy number of targeted bacteria was calculated using a standard curve.

Supplementary references

1. Kraus D, Yang Q, Kahn BB. Lipid extraction from mouse feces. *Bio Protoc* 2015;5.
2. Wu PS, Kuo YT, Chen SM, Li Y, Lou BS. Gas chromatography-mass spectrometry analysis of photosensitive characteristics in citrus and herb essential oils. *J Chromatogr Sep Tech* 2014;6.
3. Liang W, Menke AL, Driessen A, *et al.* Establishment of a general NAFLD scoring system for rodent models and comparison to human liver pathology. *PLoS One* 2014;9:e115922.
4. Purves RD. Optimum numerical integration methods for estimation of area-under-the-curve (AUC) and area-under-the-moment-curve (AUMC). *J Pharmacokinet Biopharm* 1992;20:211–26.
5. Livak KJ, Schmittgen TD. Analysis of relative gene expression data using real-time quantitative PCR and the 2(T)(-Delta Delta C) method. *Methods* 2001;25:402–408.
6. Weigmann B, Tubbe I, Seidel D, *et al.* Isolation and subsequent analysis of murine lamina propria mononuclear cells from colonic tissue. *Nat Protoc* 2007;2:2307–11.
7. Magoc T, Salzberg SL. FLASH: fast length adjustment of short reads to improve genome assemblies. *Bioinformatics* 2011;27:2957–63.
8. Caporaso JG, Kuczynski J, Stombaugh J, *et al.* QIIME allows analysis of high-throughput community sequencing data. *Nat Methods* 2010;7:335–6.
9. Bokulich NA, Subramanian S, Faith JJ, *et al.* Quality-filtering vastly improves diversity estimates from Illumina amplicon sequencing. *Nat Methods* 2013;10:57–U11.
10. Edgar RC, Haas BJ, Clemente JC, *et al.* UCHIME improves sensitivity and speed of chimera detection. *Bioinformatics* 2011;27:2194–2200.
11. Haas BJ, Gevers D, Earl AM, *et al.* Chimeric 16S rRNA sequence formation and detection in Sanger and 454-pyrosequenced PCR amplicons. *Genome Res* 2011;21:494–504.
12. Edgar RC. Search and clustering orders of magnitude faster than BLAST. *Bioinformatics* 2010;26:2460–2461.
13. Edgar RC. UPARSE: highly accurate OTU sequences from microbial amplicon reads. *Nat Methods* 2013;10:996–8.
14. DeSantis TZ, Hugenholtz P, Larsen N, *et al.* Greengenes, a chimera-checked 16S

rRNA gene database and workbench compatible with ARB. *Appl Environ Microbiol* 2006;72:5069–72.

15. McDonald D, Price MN, Goodrich J, *et al.* An improved Greengenes taxonomy with explicit ranks for ecological and evolutionary analyses of bacteria and archaea. *ISME J* 2012;6:610–8.
16. Wang Q, Garrity GM, Tiedje JM, *et al.* Naive Bayesian classifier for rapid assignment of rRNA sequences into the new bacterial taxonomy. *Appl Environ Microbiol* 2007;73:5261–7.
17. Caporaso JG, Bittinger K, Bushman FD, *et al.* PyNAST: a flexible tool for aligning sequences to a template alignment. *Bioinformatics* 2010;26:266–267.
18. Price MN, Dehal PS, Arkin AP. FastTree: computing large minimum evolution trees with profiles instead of a distance matrix. *Mol Biol Evol* 2009;26:1641–50.
19. Price MN, Dehal PS, Arkin AP. FastTree 2—approximately maximum-likelihood trees for large alignments. *PLoS One* 2010;5:e9490.
20. Lozupone C, Knight R. UniFrac: a new phylogenetic method for comparing microbial communities. *Appl Environ Microbiol* 2005;71:8228–35.
21. Lozupone C, Lladser ME, Knights D, *et al.* UniFrac: an effective distance metric for microbial community comparison. *ISME J* 2011;5:169–72.
22. White JR, Nagarajan N, Pop M. Statistical methods for detecting differentially abundant features in clinical metagenomic samples. *PLoS Computational Biol* 2009;5.
23. Chang CJ, Lin CS, Lu CC, *et al.* Ganoderma lucidum reduces obesity in mice by modulating the composition of the gut microbiota. *Nat Commun* 2015;6:7489.
24. Tang K, Pasqua T, Biswas A, *et al.* Muscle injury, impaired muscle function and insulin resistance in Chromogranin A-knockout mice. *J Endocrinol* 2017;232:137–153.
25. Ehara T, Kamei Y, Takahashi M, *et al.* Role of DNA methylation in the regulation of lipogenic glycerol-3-phosphate acyltransferase 1 gene expression in the mouse neonatal liver. *Diabetes* 2012;61:2442–50.
26. Miyata S, Inoue J, Shimizu M, *et al.* Xanthohumol improves diet-induced obesity and fatty liver by suppressing sterol regulatory element-binding protein (SREBP) Activation. *J Biol Chem* 2015;290:20565–79.
27. Shostak A, Meyer-Kovac J, Oster H. Circadian regulation of lipid mobilization in white adipose tissues. *Diabetes* 2013;62:2195–203.
28. Reid BN, Ables GP, Otlivanchik OA, *et al.* Hepatic overexpression of

hormone-sensitive lipase and adipose triglyceride lipase promotes fatty acid oxidation, stimulates direct release of free fatty acids, and ameliorates steatosis. *J Biol Chem* 2008;283:13087–99.

29. Penna F, Busquets S, Toledo M, *et al.* Erythropoietin administration partially prevents adipose tissue loss in experimental cancer cachexia models. *J Lipid Res* 2013;54:3045–51.
30. Estall JL, Kahn M, Cooper MP, *et al.* Sensitivity of lipid metabolism and insulin signaling to genetic alterations in hepatic peroxisome proliferator-activated receptor-gamma coactivator-1alpha expression. *Diabetes* 2009;58:1499–508.
31. Bu SY, Mashek MT, Mashek DG. Suppression of long chain acyl-CoA synthetase 3 decreases hepatic de novo fatty acid synthesis through decreased transcriptional activity. *J Biol Chem* 2009;284:30474–83.
32. Li G, Xie C, Lu S, *et al.* Intermittent fasting promotes white adipose browning and decreases obesity by shaping the gut microbiota. *Cell Metab* 2017;26:672–685.
33. Babkair H, Yamazaki M, Uddin MS, *et al.* Aberrant expression of the tight junction molecules claudin-1 and zonula occludens-1 mediates cell growth and invasion in oral squamous cell carcinoma. *Hum Pathol* 2016;57:51–60.
34. Muralidharan S, Ambade A, Fulham MA, *et al.* Moderate alcohol induces stress proteins HSF1 and hsp70 and inhibits proinflammatory cytokines resulting in endotoxin tolerance. *J Immunol* 2014;193:1975–87.
35. Obata T, Goto Y, Kunisawa J, *et al.* Indigenous opportunistic bacteria inhabit mammalian gut-associated lymphoid tissues and share a mucosal antibody-mediated symbiosis. *Proc Natl Acad Sci U S A* 2010;107:7419–24.

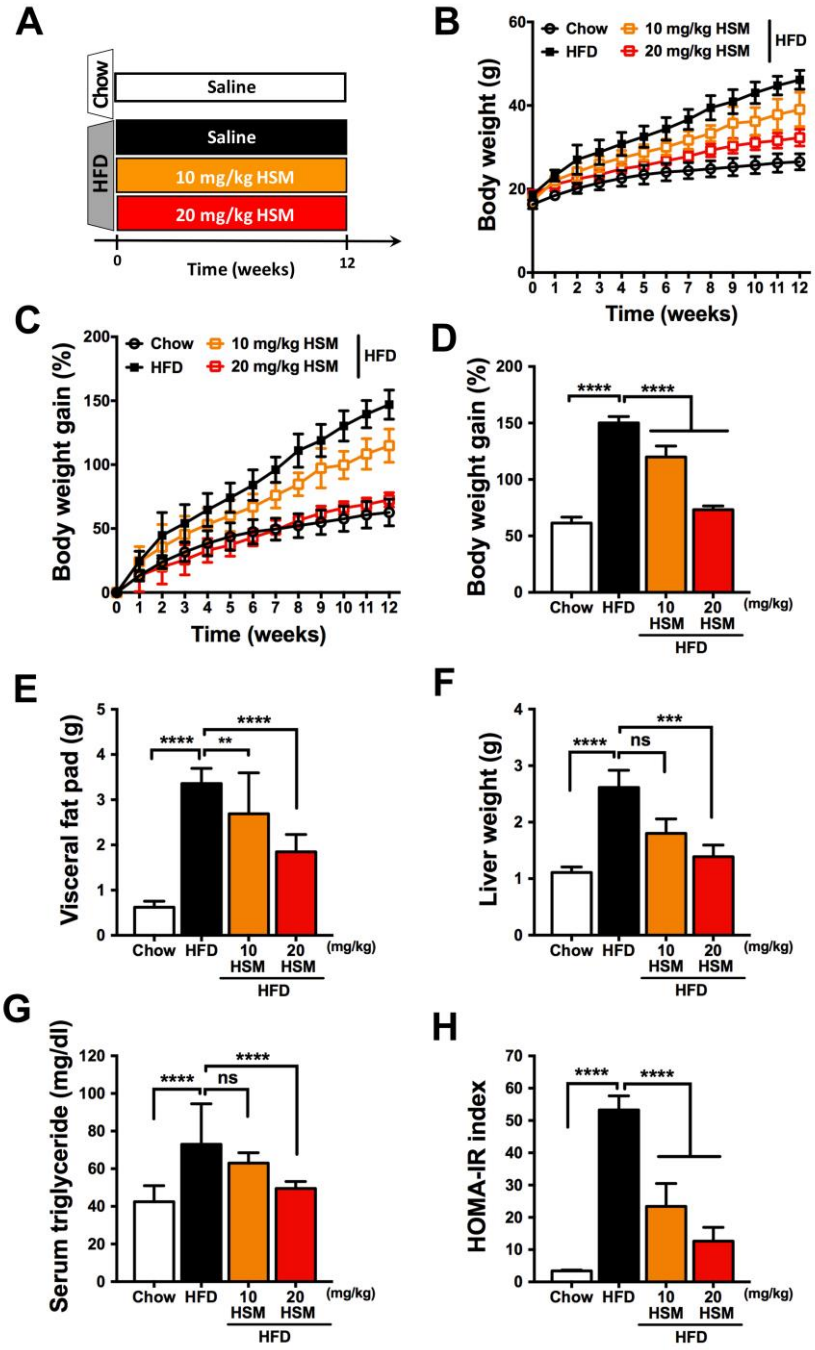

Supplementary figure S1

HSM reduces obesity in HFD-fed mice. (A) Chow-fed mice and HFD-fed mice were treated with control saline or HSM (10 or 20 mg/kg) by oral gavage for 12 weeks. (B) Body weight and (C) body weight gain were monitored throughout the 12-week period. Obesity traits including (D) body weight gain, (E) visceral fat pad weight (epididymal white adipose tissue), (F) liver weight, (G) serum triglycerides and (H) HOMA-IR index were assessed after 12 weeks of treatments. Data are presented as means ± SD. n=14 to 15 for panels B–E; n=9 to 10 for panels F,G. Data were analyzed using one-way ANOVA followed by Bonferroni's post hoc test. **p<0.01; ***p<0.001; ns, not significant.

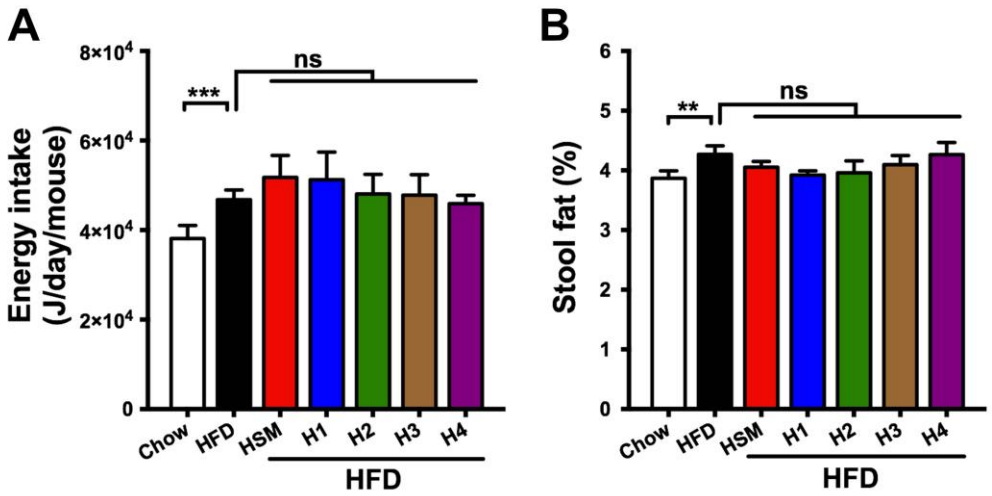

Supplementary figure S2

HSM and polysaccharide fractions do not affect energy intake or lipid absorption in HFD-fed mice. Experiments were performed as in figure 1. Fractions H1–H4 were given at 20 mg/kg by oral gavage for 12 weeks. (A) Average daily energy intake (n=10 mice/group). (B) Fecal lipid content. Data are shown as means ± SD (n=5 mice/group). Data were analyzed using one-way ANOVA followed by Bonferroni's post hoc test. **p<0.01; ***p<0.001; ns, not significant.

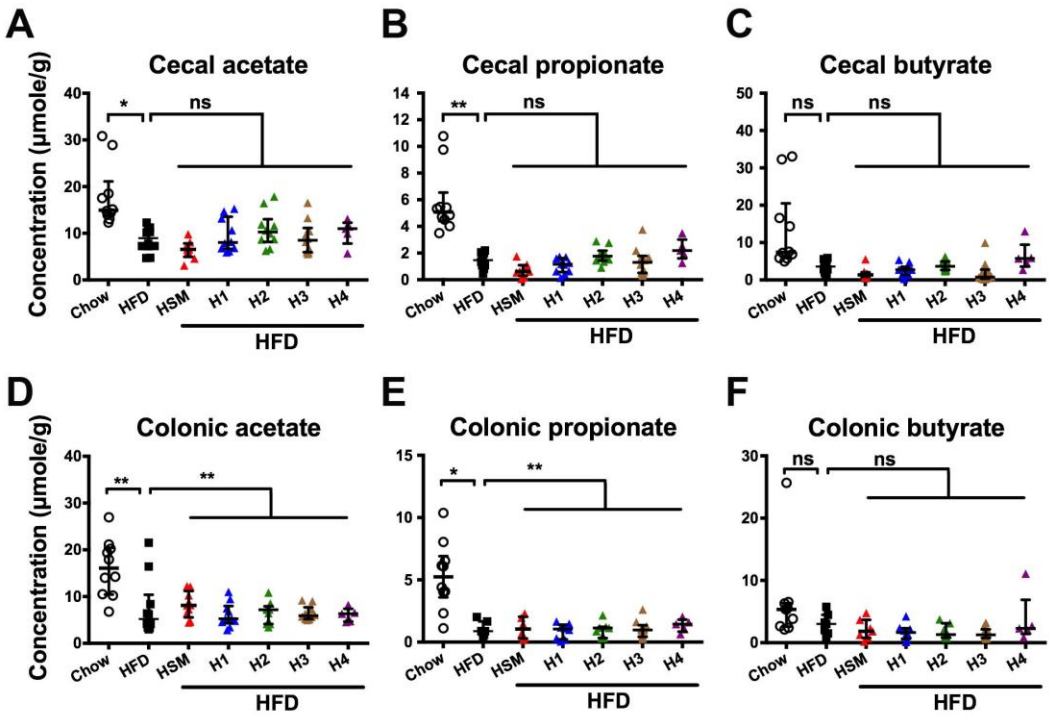

Supplementary figure S3

HSM and polysaccharide fractions do not affect intestinal production of short chain fatty acids. Experiments were performed as in figure 1. Acetate, propionate and butyrate were quantified in (A–C) cecum or (D–F) colon of chow-fed and HFD-fed mice after 12 weeks of treatment. Data represent medians ± interquartile range (IQR) (n=5 to 10 mice/group). Data were analyzed using Kruskal-Wallis test with Dunn's post hoc test. *p<0.05; **p<0.01; ns, not significant.

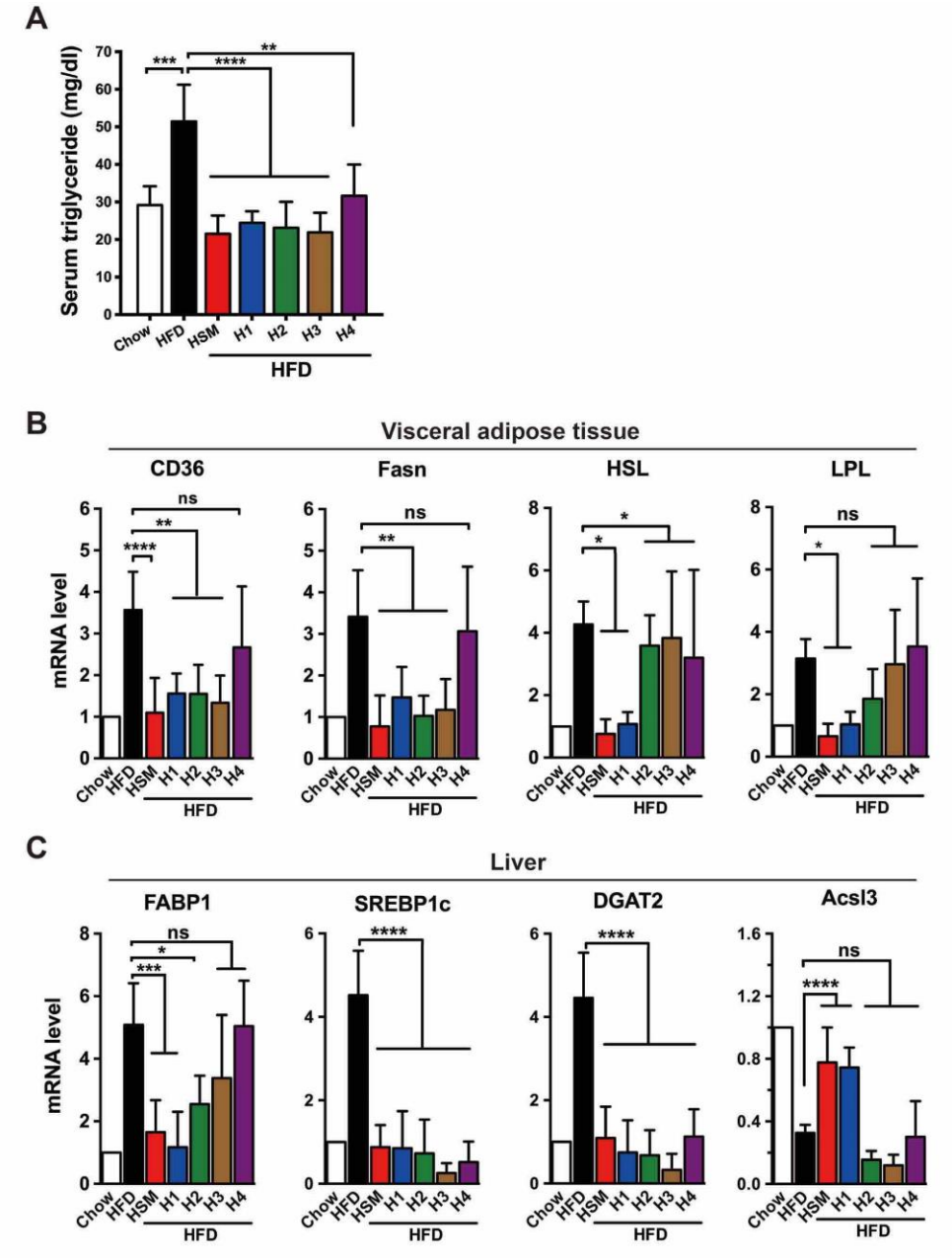

Supplementary figure S4

Effects of HSM and polysaccharide fractions on serum triglycerides and gene expression involved in lipid metabolism. Experiments were performed as in figure 1. (A) Serum triglycerides (n=5 per group). qRT-PCR analysis of lipid metabolism genes in (B) visceral adipose and (C) hepatic tissues. The genes examined are involved in lipid transport and uptake (cluster of differentiation 36, CD36; fatty acid-binding protein 1, FABP1), lipogenesis (diglyceride acyltransferase, DGAT2; fatty acid synthase, Fasn; sterol regulatory-element binding protein 1c, SREBP1c), lipolysis (hormone-sensitive lipase, HSL; lipoprotein lipase, LPL) or β-oxidation (long-chain-fatty-acid-CoA ligase 3, Acsl3). Data represent means ± SD (n=5 to 10 mice/group). Data were analyzed using one-way ANOVA followed by Bonferroni's post hoc test. *p<0.05; **p<0.01; ***p<0.001; ****p<0.0001; ns, not significant.

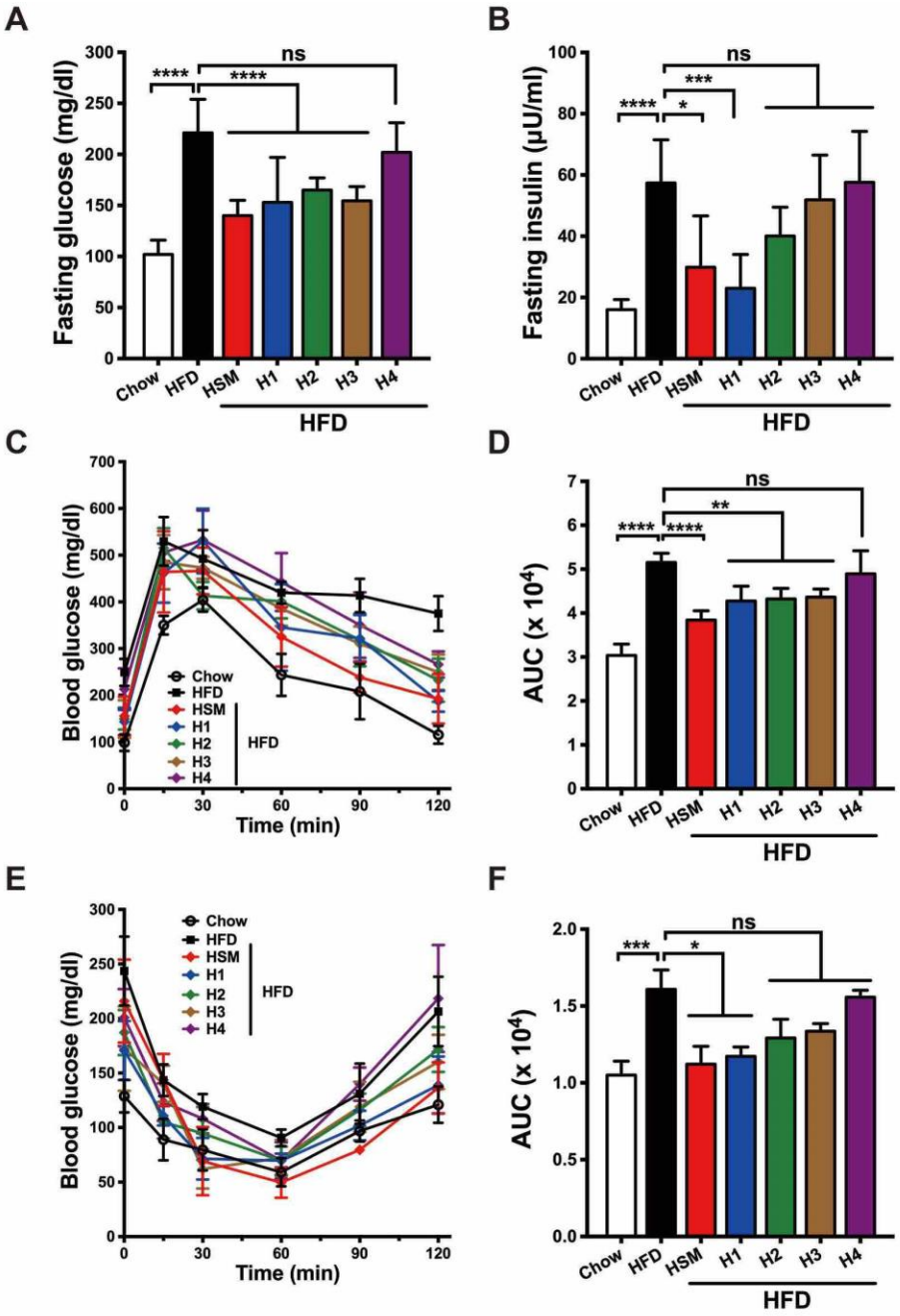

Supplementary figure S5

HSM and H1 restore glucose and insulin sensitivity in HFD-induced obese mice. Experiments were performed as in figure 1. (A) Fasting blood glucose and (B) fasting serum insulin. (C) OGTT and (D) the corresponding area under the curve (AUC). (E) ITT and (F) the corresponding AUC values. Data represent means ± SD (n=10 to 15 mice for panels A,B; n=5 for panels C–F) and analyzed using one-way ANOVA followed by Bonferroni's post hoc test. *p<0.05; **p<0.01; ***p<0.001; ****p<0.0001; ns, not significant.

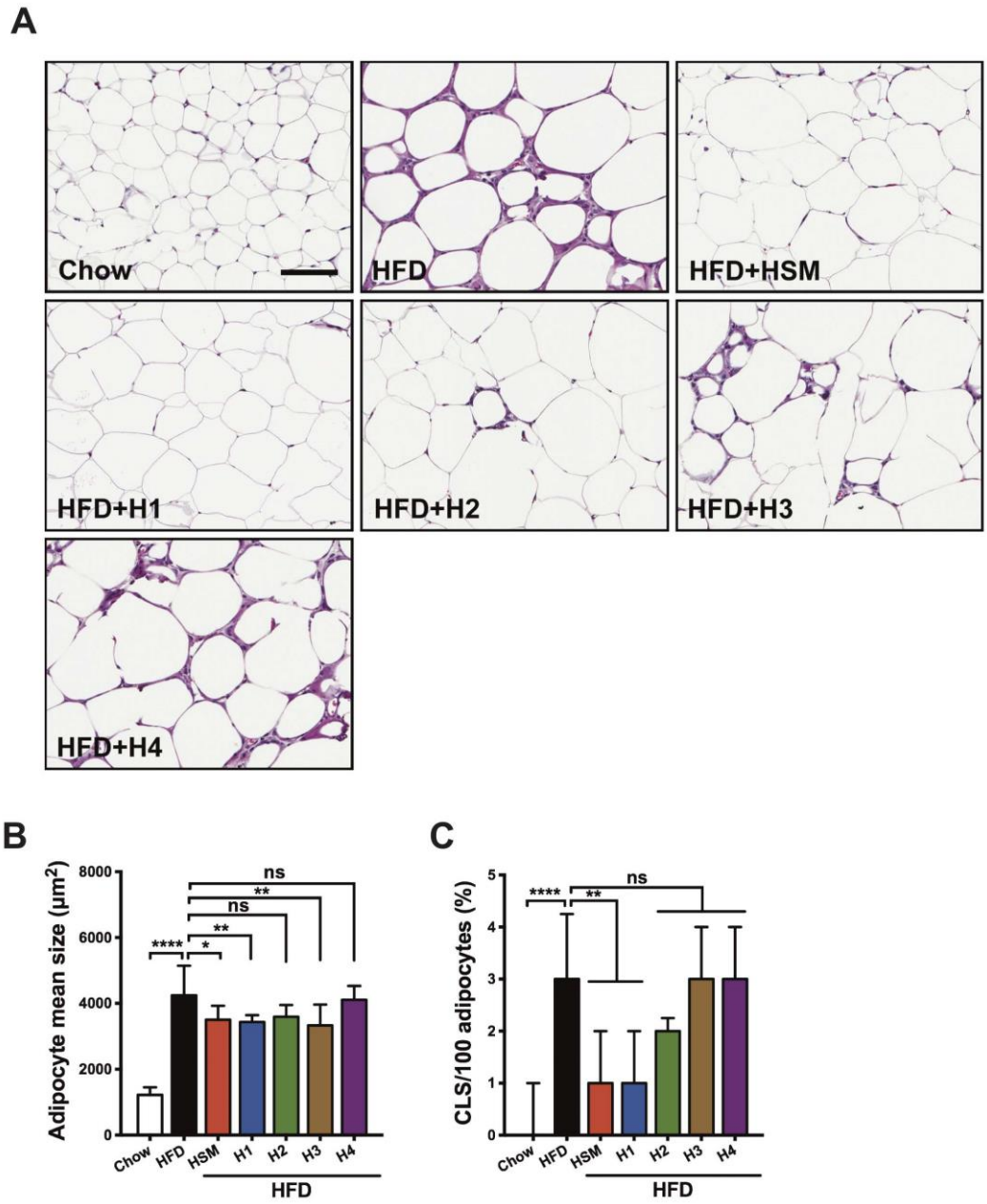

Supplementary figure S6

HSM and H1 reduce adipocyte hypertrophy and crown-like structures in HFD-fed mice. Experiments were performed as in figure 1. (A) Representative images of hematoxylin and eosin (H&E)-stained visceral adipose tissues. Scale bar, 100 µm. (B) Adipocyte size in visceral adipose tissues was determined from five microscopy fields for each mouse using Adiposoft (Image J). Data represent medians ± IQR (n=10 mice/group). Data were analyzed using the Kruskal-Wallis test with Dunn's post hoc test. (C) Quantification of crown-like structures (CLS; n=5 images per mouse) in visceral adipose tissues. Data represent means ± SD (n=10 mice/group). Data were analyzed using one-way ANOVA followed by Bonferroni's post hoc test. *p<0.05; **p<0.01; ***p<0.001; ****p<0.0001; ns, not significant.

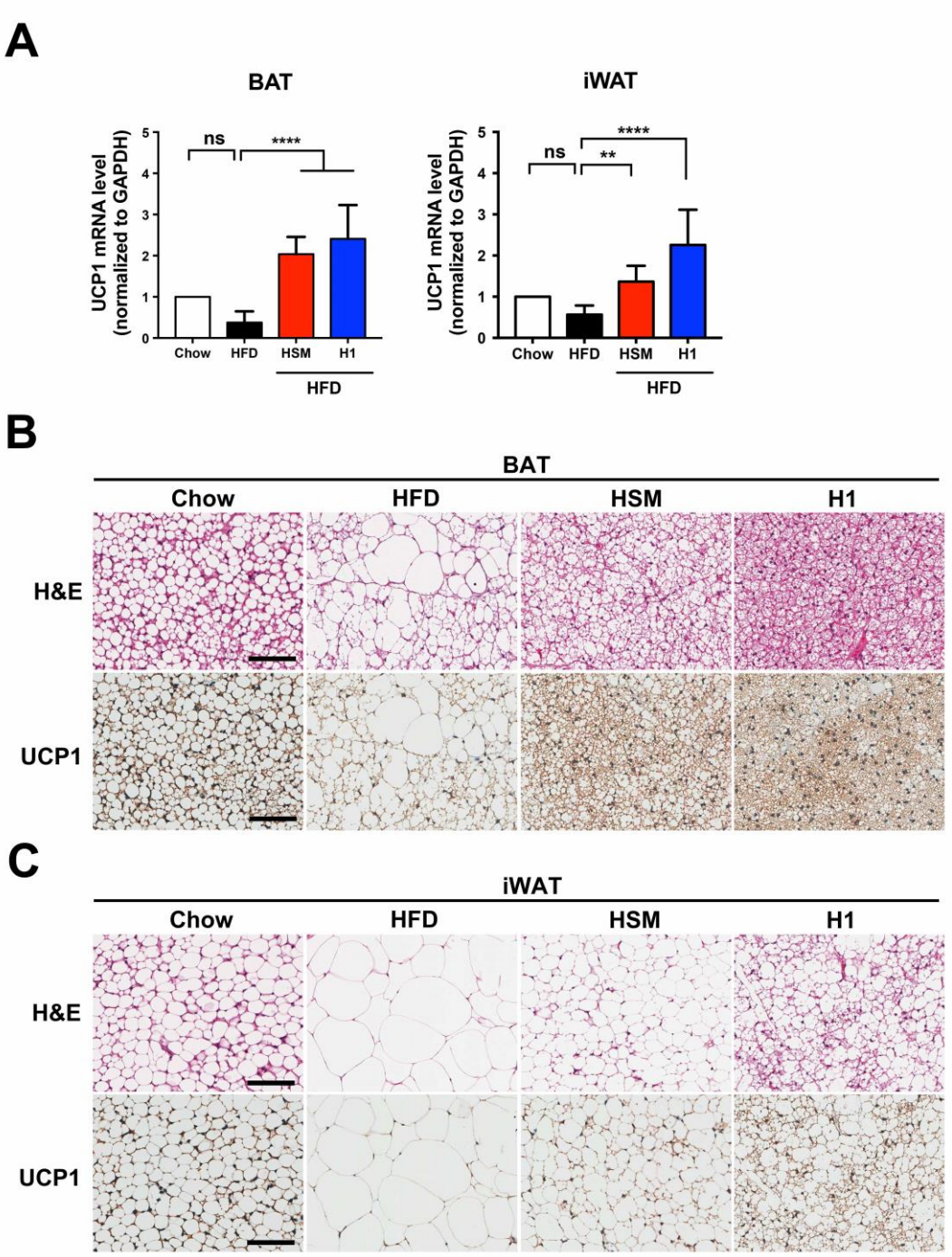

Supplementary figure S7

HSM and H1 induce expression of thermogenic protein markers in HFD-fed mice. (A) Quantitative real-time-PCR (qRT-PCR) analysis of mitochondrial uncoupling protein 1 (UCP1) gene expression in brown adipose tissues (BATs, left panel) and inguinal white adipose tissues (iWATs, right panel). Representative images of H&E-stained and UCP1-stained (B) BATs and (C) iWATs. Tissue slides that were cut in succession were used. Scale bars, 100 µm. Data represent means ± SD (n=5 mice/group). Data were analyzed using one-way ANOVA followed by Bonferroni's post hoc test. **p<0.01; ****p<0.0001; ns, not significant.

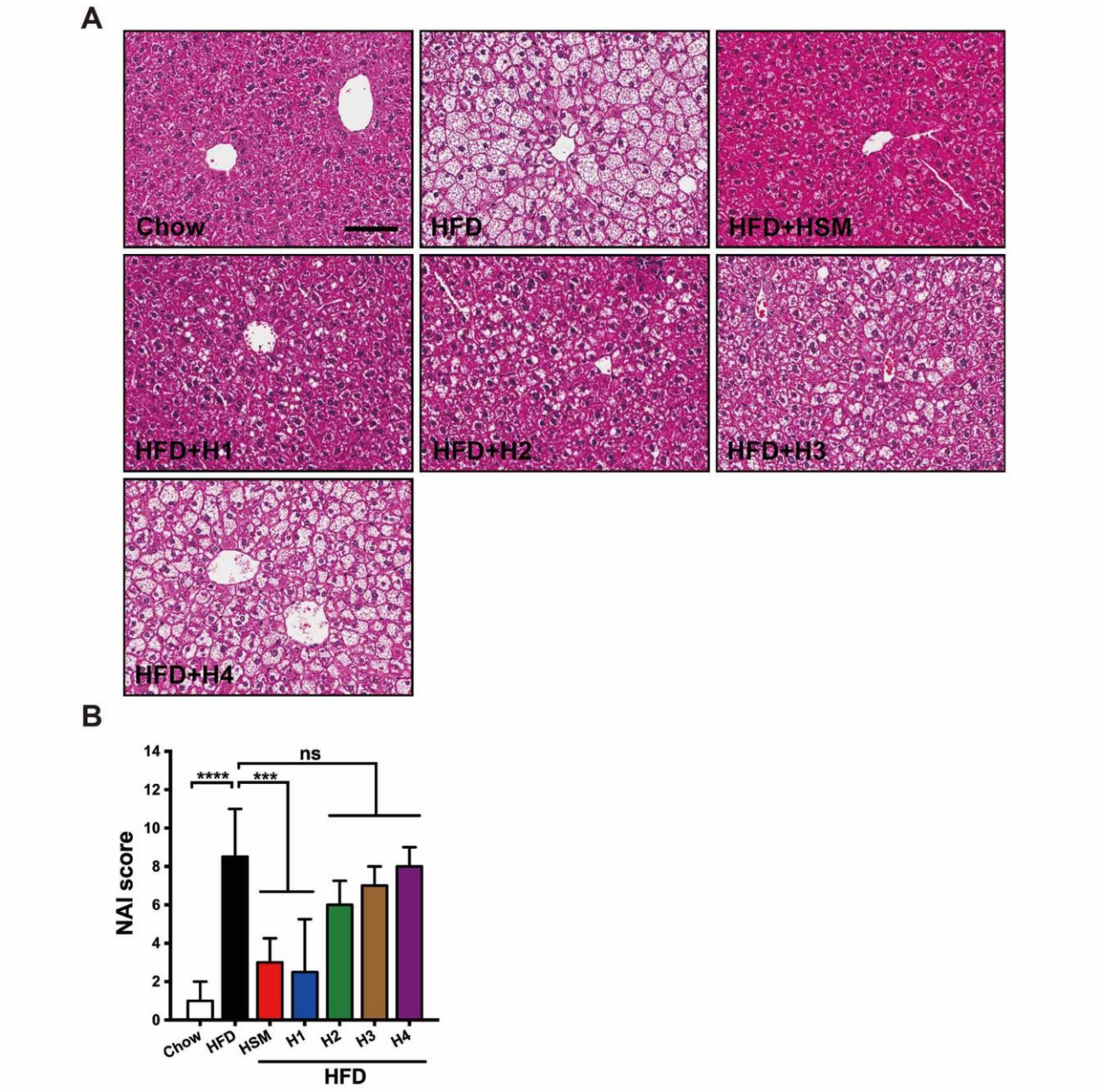

Supplementary figure S8

HSM and H1 reduce pathological signs of NAFLD and NASH in HFD-fed mice. Experiments were performed as in figure 1. (A) Representative images of H&E-stained liver tissues. Scale bar, 100 µm. (B) Non-alcoholic steatohepatitis (NASH) activity index (NAI; n=5 images per mouse). Data represent means ± SD (n=10 mice per group) and analyzed using one-way ANOVA followed by Bonferroni's post hoc test. ***p<0.001; ****p<0.0001; ns, not significant.

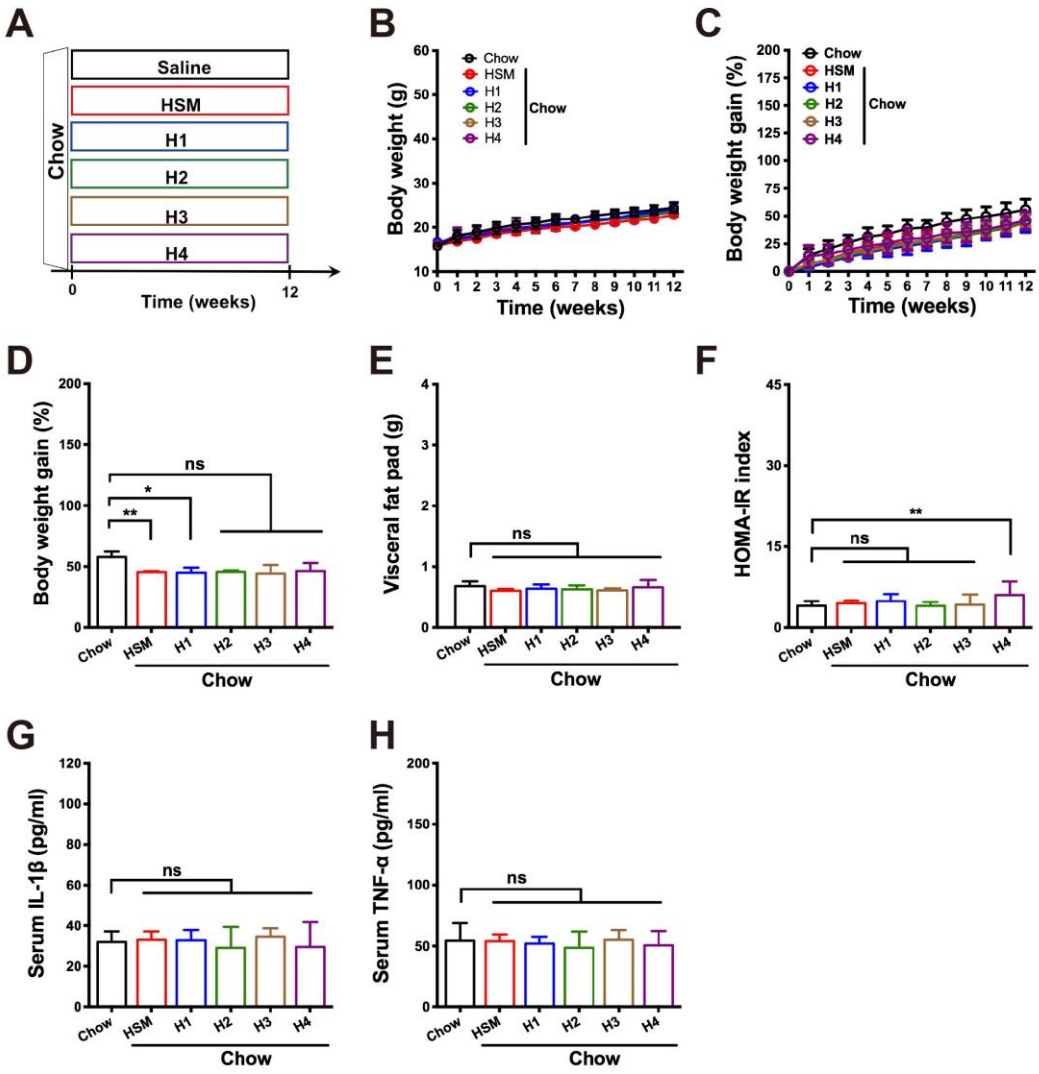

Supplementary figure S9

Effects of HSM and H1 treatment in chow-fed mice. (A) Chow-fed mice were treated daily with saline, HSM or fractions H1–H4 for 12 weeks as indicated. (B) Body weight was monitored for 12 weeks. Obesity traits including (C) body weight gain, (D) visceral fat pad weight, (E) HOMA-IR index, (F) serum IL-1β, and (G) serum TNF-α were measured after 12 weeks of treatments as described in Methods. Data are presented as means ± SD. n=10 to 15 mice/group for panels A–C,E; n=5 to 10 mice/group for panels D,F,G. Statistical analysis was performed using one-way ANOVA followed by Bonferroni's post hoc test. *p<0.05; **p<0.01; ns, not significant.

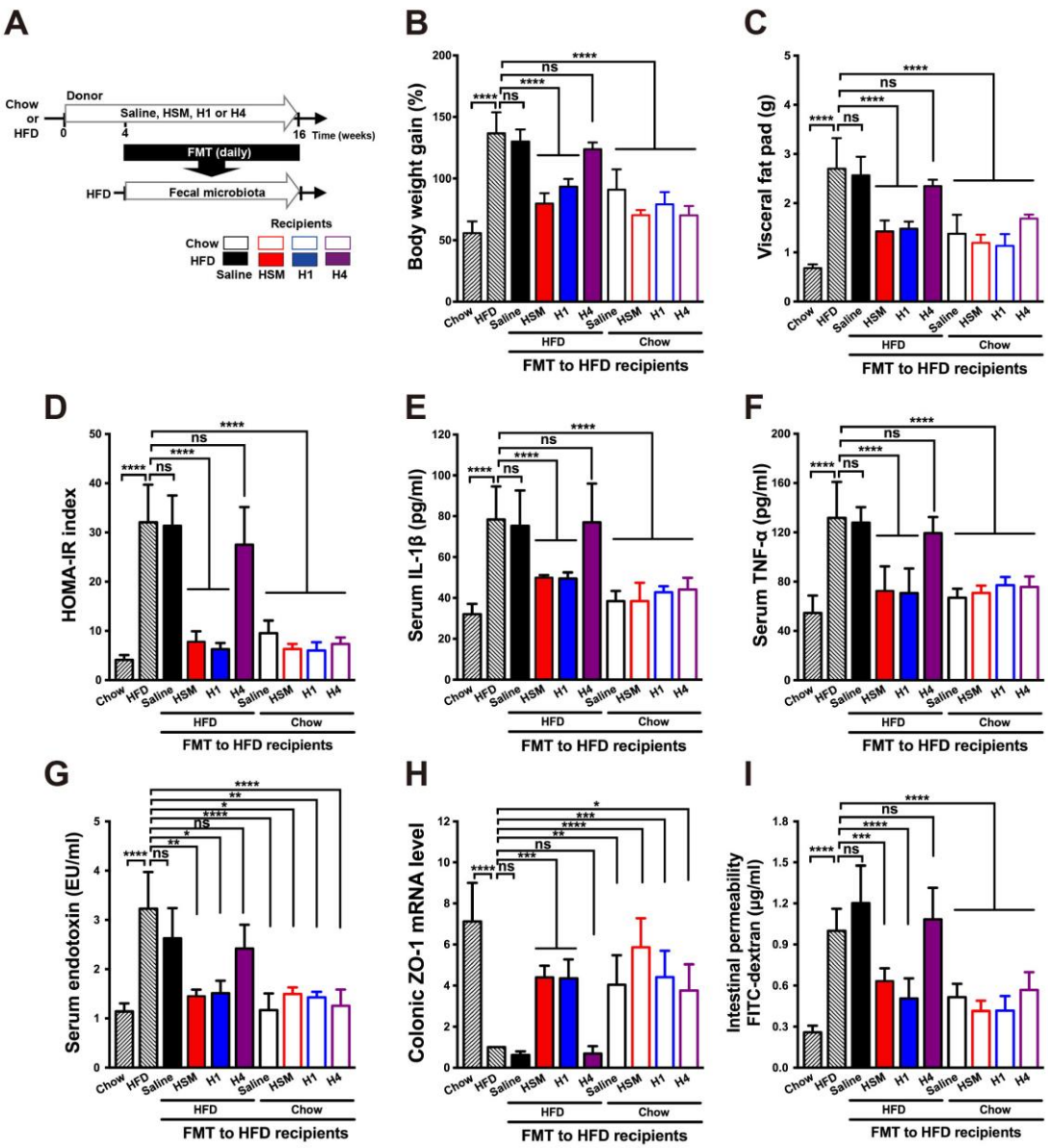

Supplementary figure S10

FMT from HSM- and H1-treated mice reduces obesity and metabolic disorders in HFD-fed recipient mice. (A) Diagram illustrating the horizontal FMT experiments performed. HFD-fed mice were treated with fecal microbiota from chow-fed donors or HFD-fed donors treated with saline, HSM, H1 or H4. Obesity traits consisting of (B) body weight gain, (C) visceral fat pad weight, (D) HOMA-IR index, (E) serum IL-1β, (F) serum TNF-α, (G) serum endotoxin, (H) colonic ZO-1 mRNA expression and (I) intestinal permeability were measured after 12 weeks of FMT. Data are presented as means ± SD and analyzed using one-way ANOVA followed by Bonferroni's post hoc test and false-discovery rate (FDR) correction for multiple testing. n=10 to 15 mice/group for panels B–G; n=5 to 15 mice/group for panels H–I. *p<0.05; **p<0.01; ***p<0.001; ****p<0.0001; ns, not significant.

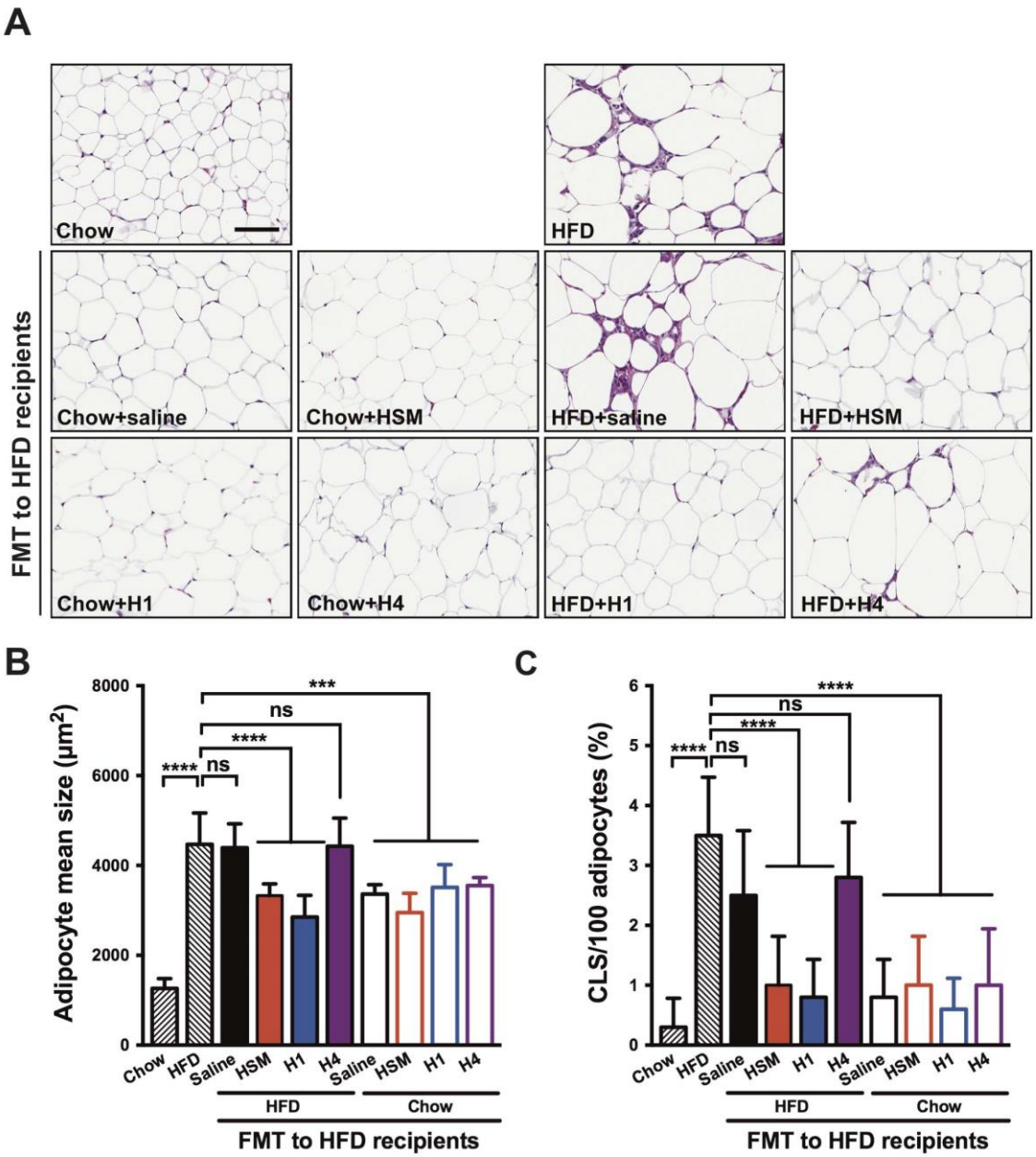

Supplementary figure S11

FMT from HSM- and H1-treated mice reduces adipocyte hypertrophy and crown-like structures in HFD-fed mice. Experiments were performed as in supplementary figure 10. (A) Representative images of H&E-stained visceral adipose tissues. Scale bar, 100 µm. (B) Mean adipocyte size in visceral adipose tissues was determined from five microscopy fields for each mouse using Adiposoft (Image J). Data represent medians ± IQR (n=10 mice/group). Data were analyzed using the Kruskal-Wallis test with Dunn's post hoc test. (C) Quantification of crown-like structures (CLS; n=5 images per mouse) in visceral adipose tissues. Data represent means ± SD (n=10 mice/group). Data were analyzed using one-way ANOVA followed by Bonferroni's post hoc test. ***p<0.001; ****p<0.0001; ns, not significant.

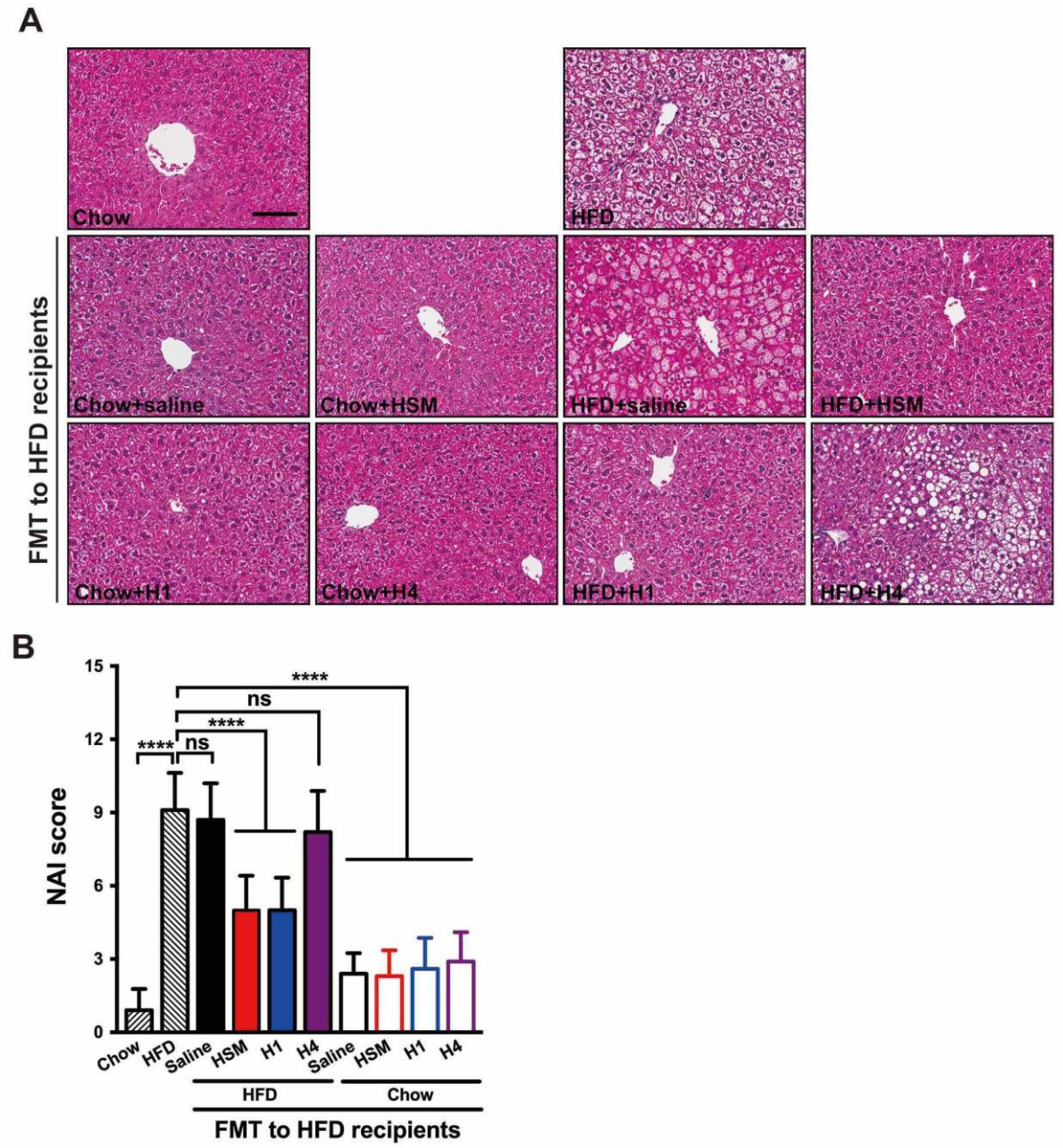

Supplementary figure S12

FMT from HSM- and H1-treated mice reduces NAFLD and NASH pathological changes. Experiments were performed as in supplementary figure 10. (A) Representative images of H&E-stained liver tissues. Scale bar, 100 µm. (B) NASH activity index (NAI; n=5 images per mouse). Data represent means ± SD (n=10 mice/group) analyzed using one-way ANOVA followed by Bonferroni's post hoc test. ****p<0.0001; ns, not significant.

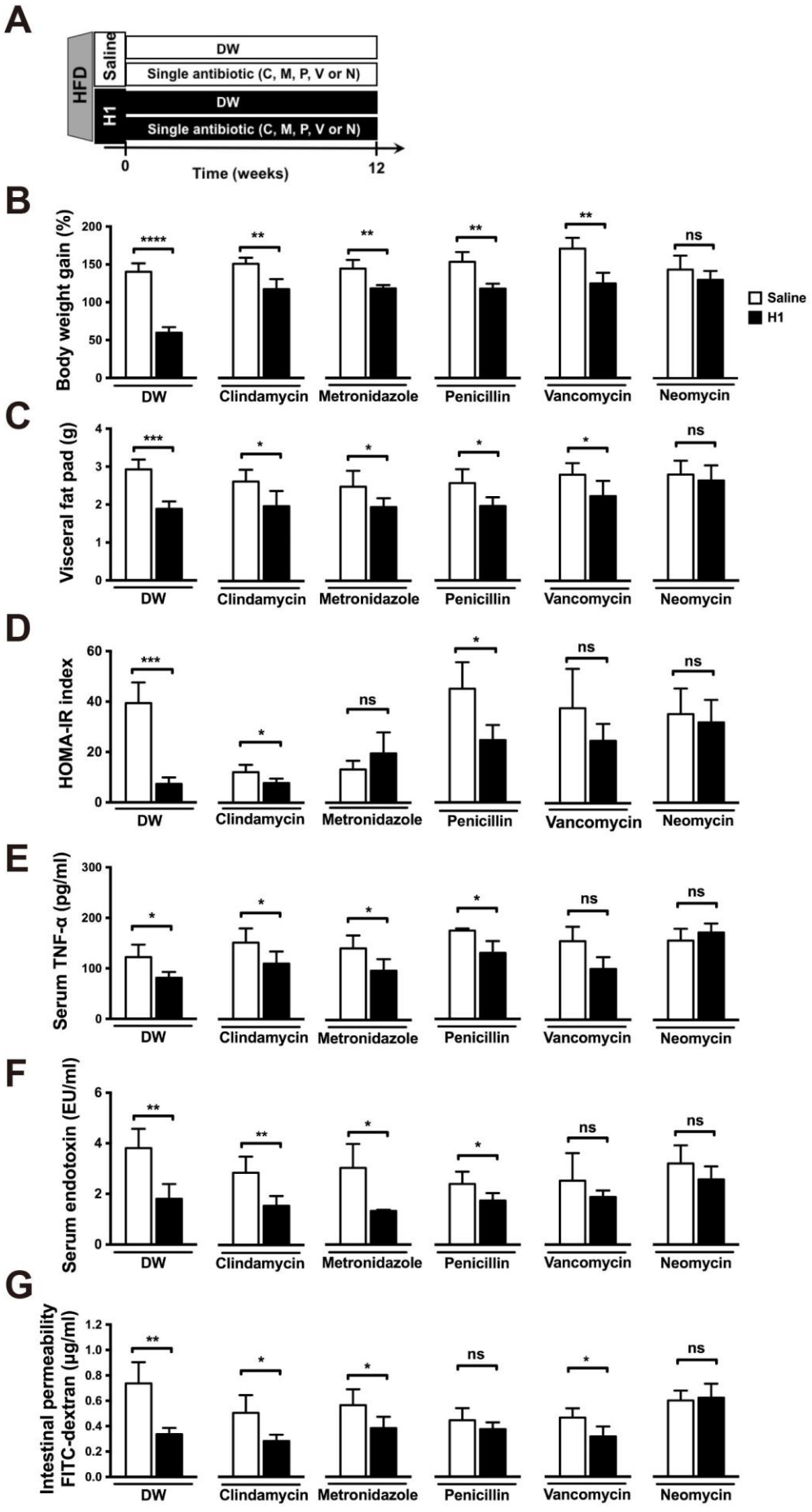
A
HFD
Saline
H1
DW
Single antibiotic (C, M, P, V or N)
DW
Single antibiotic (C, M, P, V or N)
0
Time (weeks)
12
B
Body weight gain (%)
C
Visceral fat pad (g)
D
HOMA-IR index
E
Serum TNF-α (pg/ml)
F
Serum endotoxin (EU/ml)
G
Intestinal permeability
FITC-dextran (μg/ml)
Saline
H1
DW
Clindamycin
Metronidazole
Penicillin
Vancomycin
Neomycin
ns

Supplementary figure S13

Neomycin treatment abrogates H1-mediated anti-obesogenic effects. (A) Diagram illustrating the single antibiotic treatment model used in these experiments. Saline- or H1-treated HFD-fed mice were treated with individual antibiotics in sterile drinking water (DW) for 12 weeks. Obesity traits including (B) body weight gain, (C) visceral fat pad weight, (D) HOMA-IR index, (E) serum TNF-α, (F) serum endotoxin and (G) intestinal permeability were measured after 12 weeks of treatment. Data are presented as means ± SD (n=5 mice/group) and analyzed using Student's unpaired t-test and FDR correction for multiple testing. *p<0.05; **p<0.01; ***p<0.001; ****p<0.0001; C, clindamycin; M, metronidazole; N, neomycin; ns, not significant; P, penicillin; V, vancomycin.

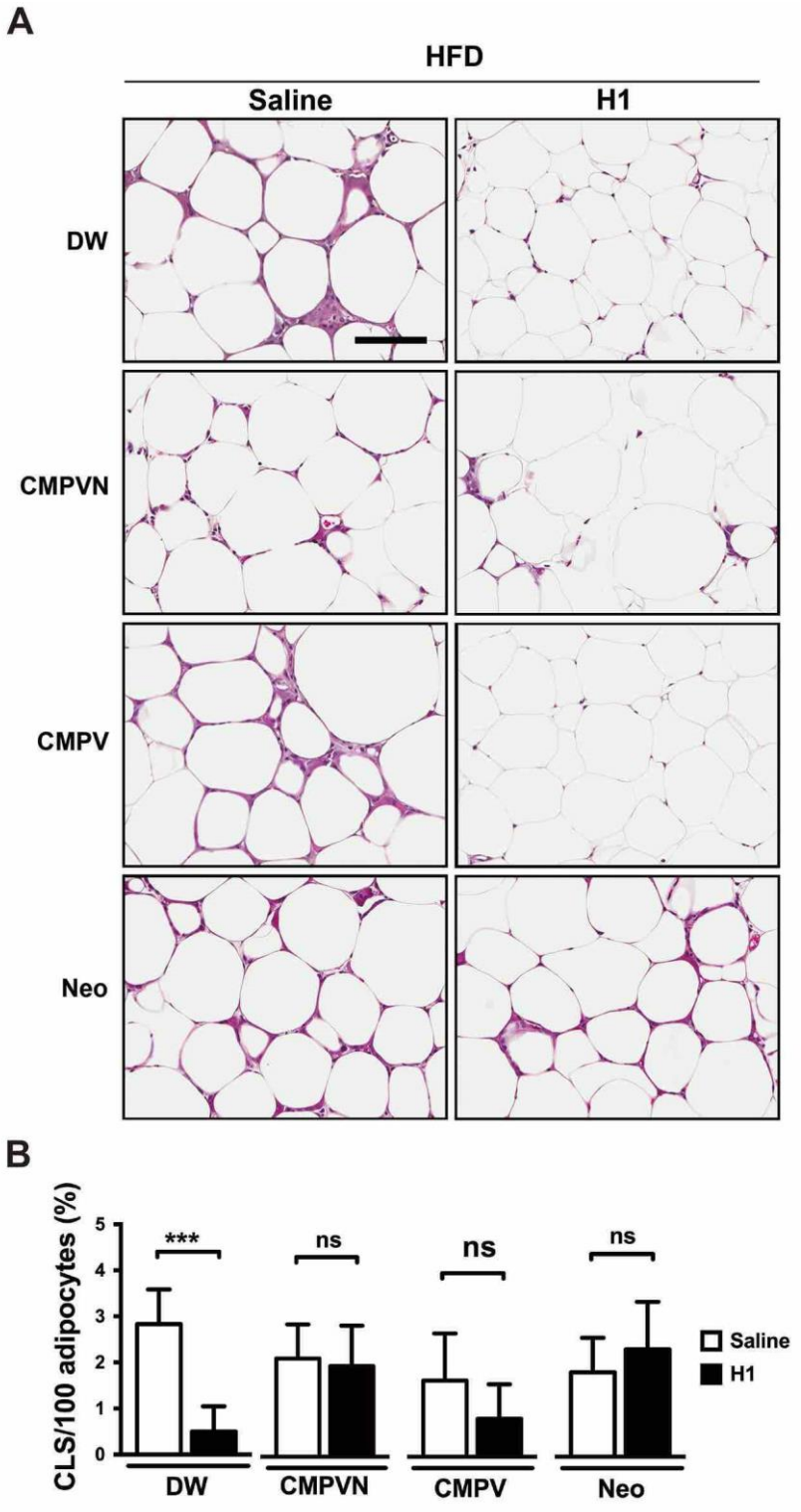

Supplementary figure S14

Neomycin treatment abrogates H1's protective effects on adipocyte hypertrophy and crown-like structures in HFD-fed mice. Experiments were performed as in figure 3. (A) Representative images of H&E-stained visceral adipose tissues. Scale bar, 100 µm. (B) Quantification of CLS (n=5 images/mouse) in visceral adipose tissues. Data represent means ± SD (n=6 mice/group) analyzed using one-way ANOVA followed by Bonferroni's post hoc test. ***p<0.001; ns, not significant.

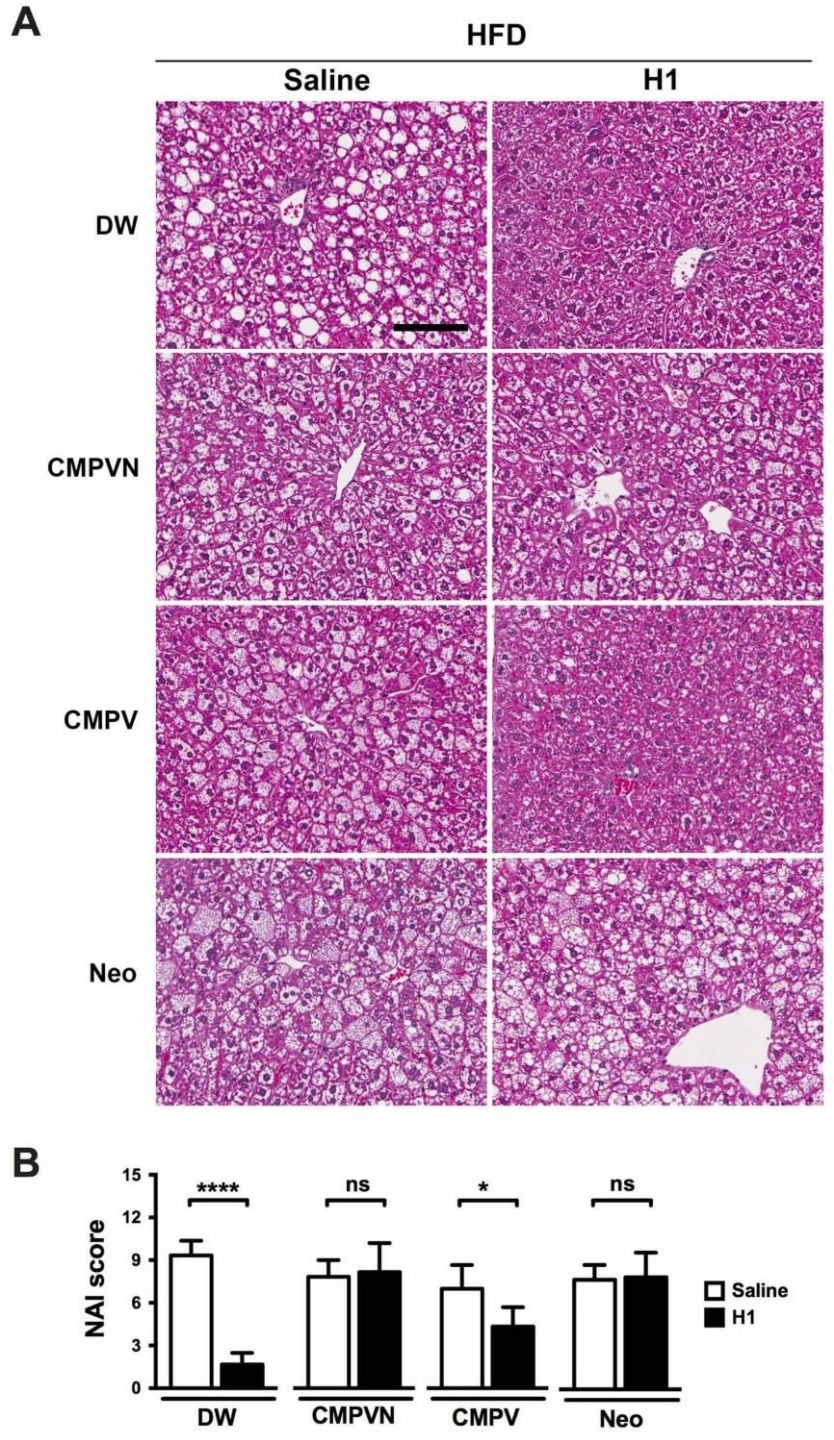

Supplementary figure S15

Neomycin treatment abrogates H1's protective effects on NAFLD and NASH in HFD-fed mice. Experiments were performed as in figure 3. (A) Representative images of H&E-stained liver tissues. Scale bar, 100 µm. (B) NAI score (n=5 images/mouse). Data represent means ± SD (n=6 mice/group) analyzed using one-way ANOVA followed by Bonferroni's post hoc test. ****p<0.0001; ns, not significant.

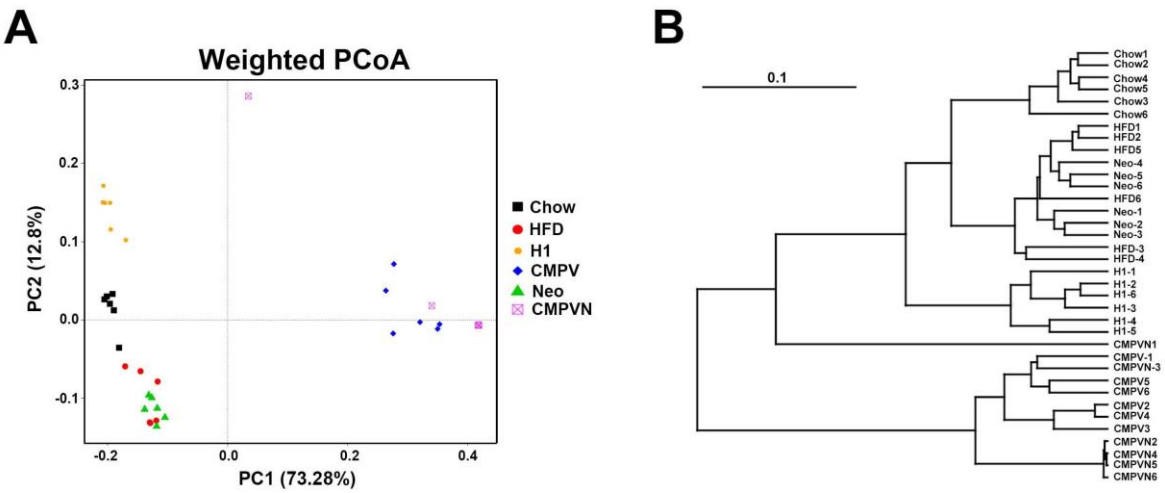

Supplementary figure S16

Clustering of gut microbiota samples based on next-generation 16S rDNA sequencing analysis. Experiments were performed as in figure 4A. (A) Plots of weighted UniFrac PCoA was prepared based on OTU abundance matrix. (B) Weighted UPGMA hierarchical clustering based on UniFrac distances (n=6 mice/group).

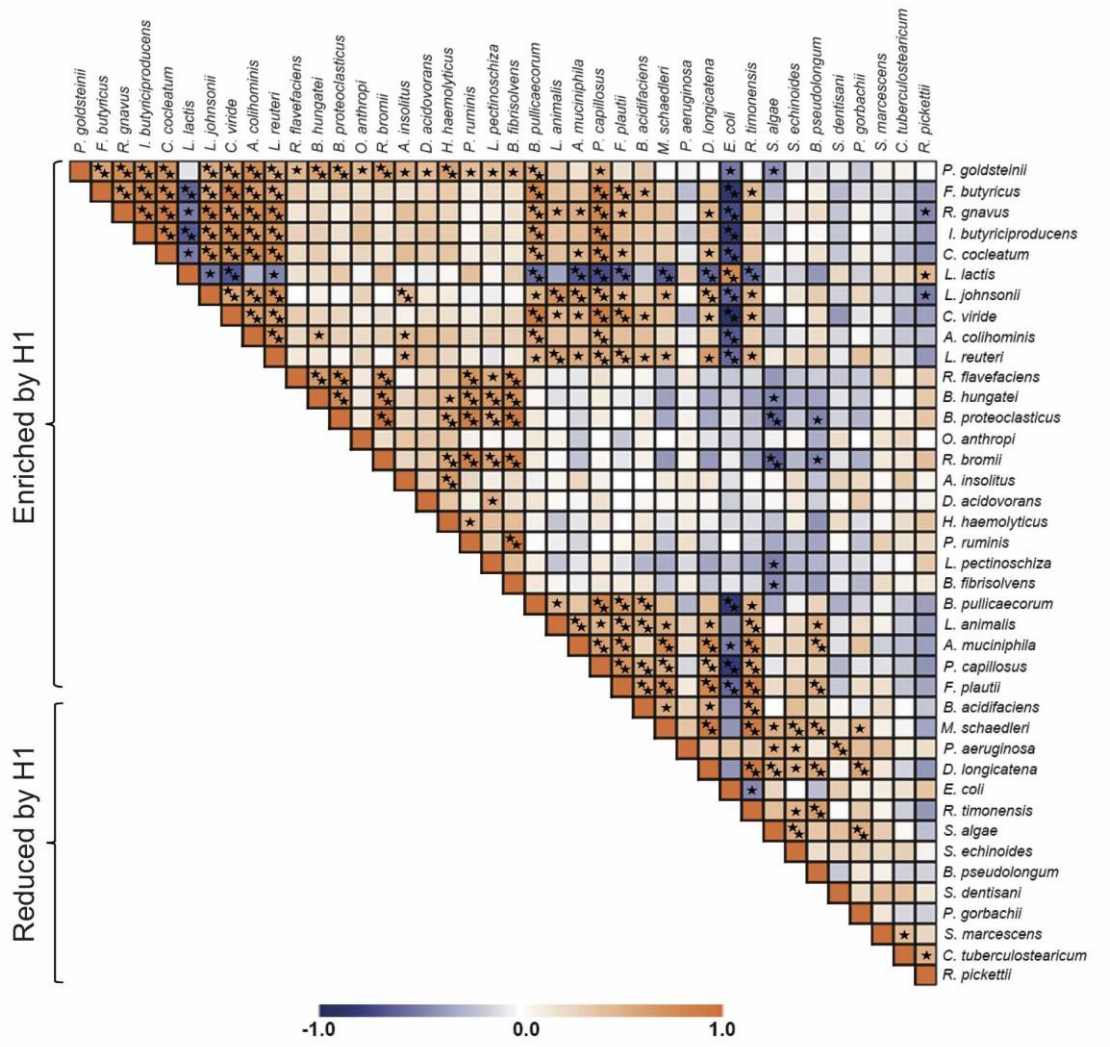

Supplementary figure S17

Interplay between H1-modulated gut bacteria. Experiments were performed as in figure 4A. Spearman correlation analysis of 40 H1-modulated gut bacterial species. Black stars indicate statistically significant difference based on Spearman correlation analysis. FDR correction for multiple testing was used. *p<0.05; ** p<0.01.

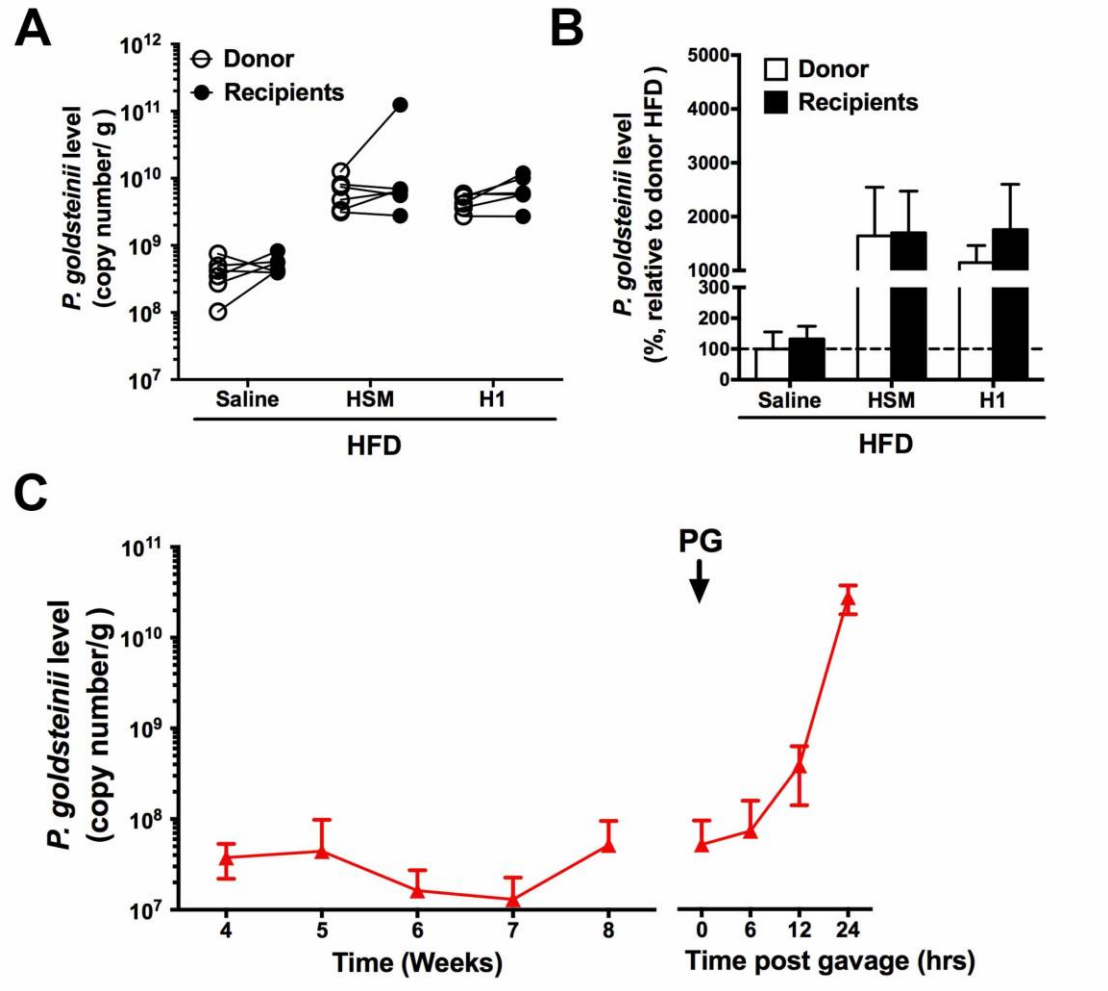

Supplementary figure S18

P. goldsteinii colonizes mice in FMT experiments. Experiments were performed as in supplementary figure S10. (A) *P. goldsteinii* levels in cecal microbiota of HFD-fed mice treated with saline, HSM or H1 and their recipients were quantified. (B) Relative levels of *P. goldsteinii* in feces of donor and recipient mice were calculated based on levels found in HFD-fed donors. (C) Colonization efficiency after a single oral gavage of *P. goldsteinii* in HFD-fed mice treated with neomycin (red line). Data are presented as means ± SD (n=5 mice/group).

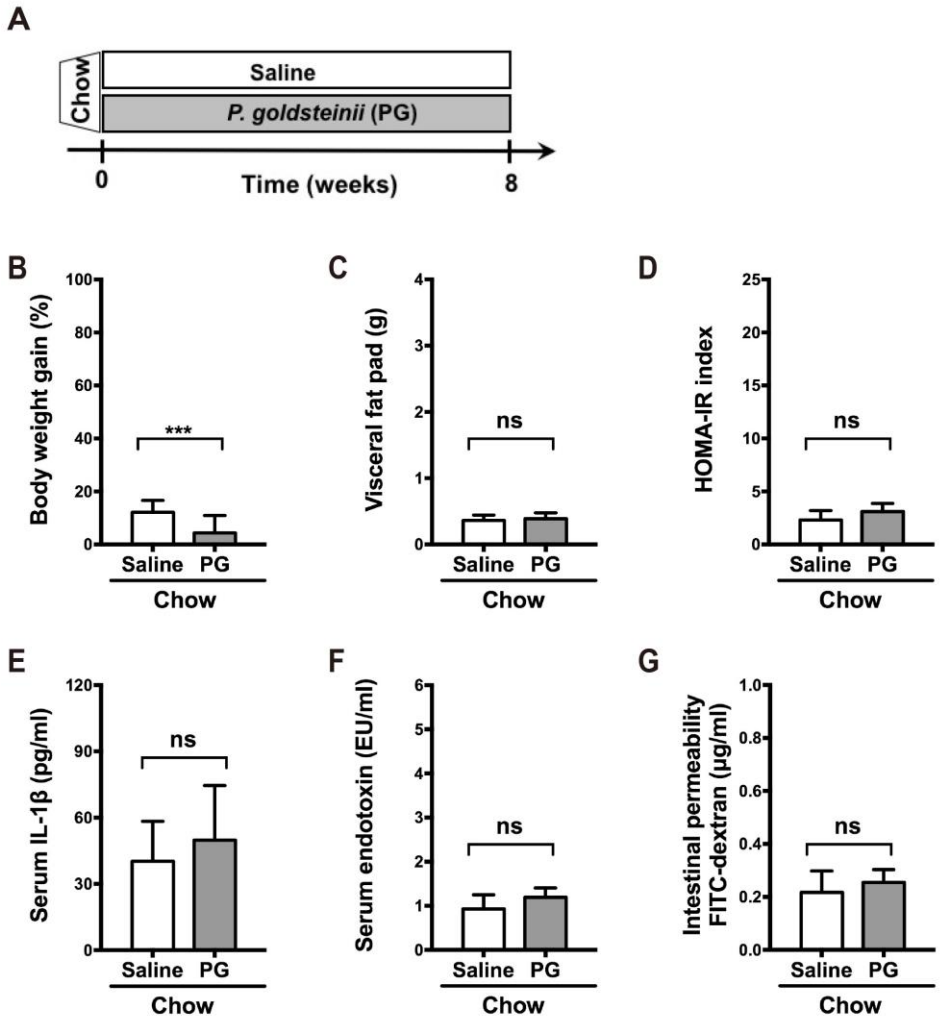

Supplementary figure S19

Effects of *P. goldsteinii* treatment in chow-fed mice. (a) Chow-fed mice were treated daily with saline or *P. goldsteinii* (PG, 4×10^7 CFUs) by oral gavage for 8 weeks. Obesity traits including (B) body weight gain, (C) visceral fat pad weight, (D) HOMA-IR index, (E) serum IL-1β, (F) serum endotoxin and (G) intestinal permeability were measured after 8 weeks of treatments. Data represent means ± SD. n=19 mice/group for panels B,C; n=6 mice/group for panels D,F,G; n=11 for panel E. Data were analyzed using one-way ANOVA followed by Bonferroni's post hoc test. ***p<0.001; ns, not significant.

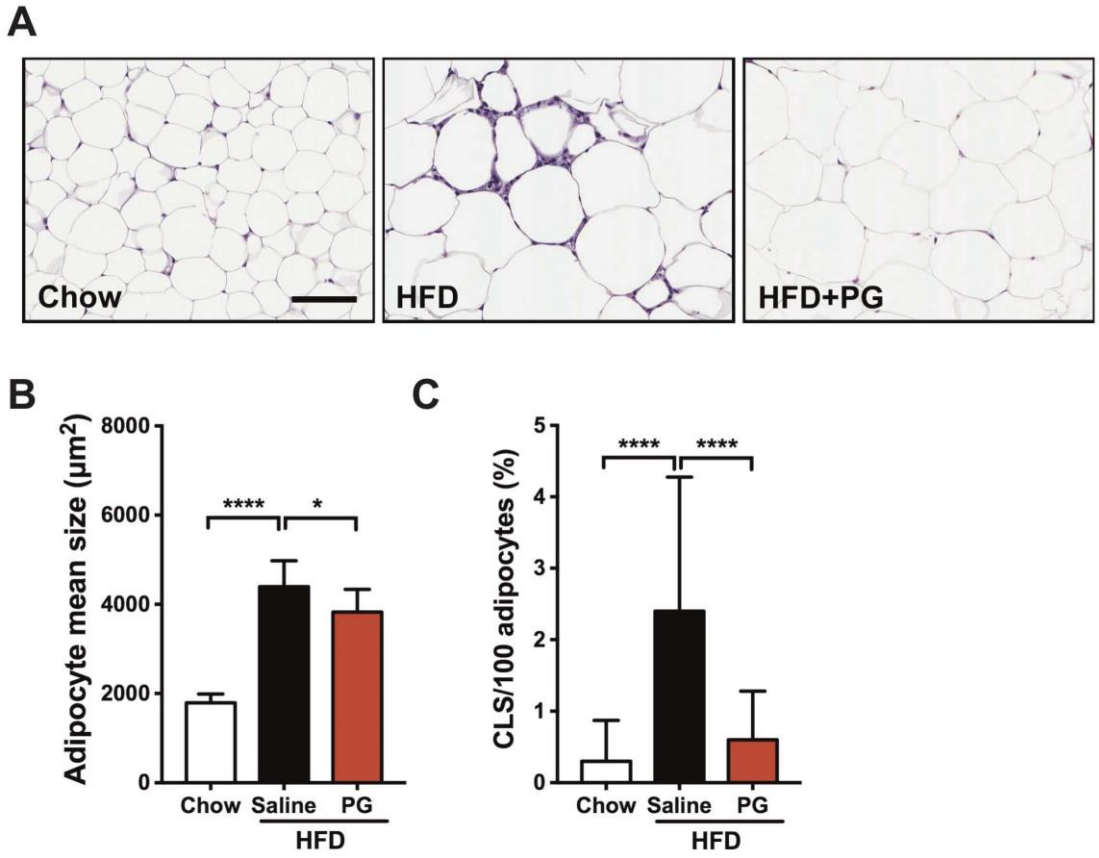

Supplementary figure S20

P. goldsteinii treatment prevents hypertrophy and crown-like structures in adipocytes of HFD-fed mice. Experiments were performed as in figure 7. (A) Representative images of H&E-stained visceral adipose tissues. Scale bar, 100 µm. (B) Adipocyte size in visceral adipose tissues was determined from five microscopy fields for each mouse using Adiposoft (Image J). Data represent medians ± IQR (n=5 mice/group). Data were analyzed using the Kruskal-Wallis test with Dunn's post hoc test. (C) Quantification of CLS (n=5 images/mouse) in visceral adipose tissues. Data represent means ± SD (n=5 mice/group). Data were analyzed using one-way ANOVA followed by Bonferroni's post hoc test. **p<0.01; ****p<0.0001.

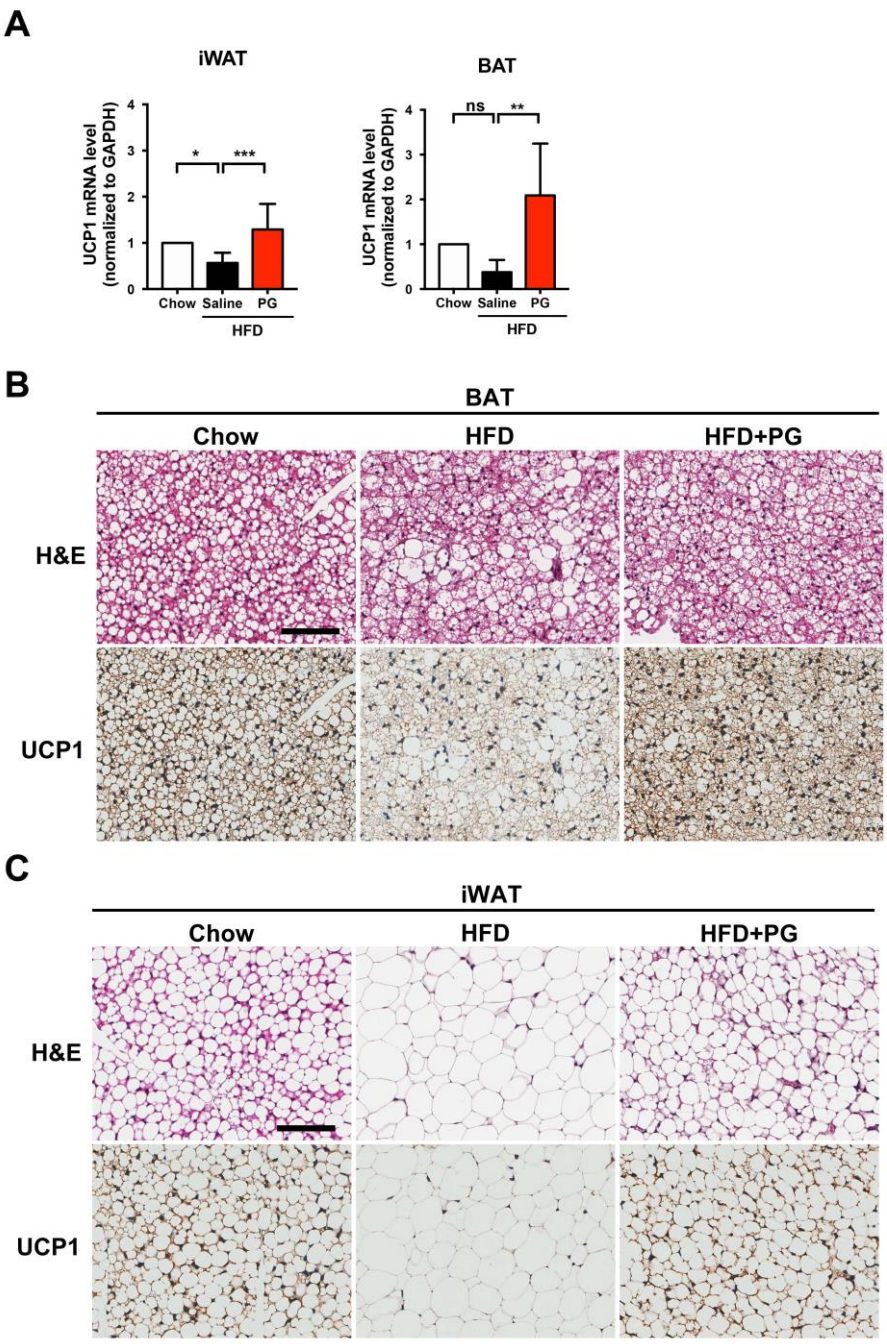

Supplementary figure S21

Live *P. goldsteinii* induces expression of thermogenic protein markers in HFD-fed mice. (A) qRT-PCR analysis of uncoupling protein 1 (UCP1) gene in BATs (left panel) and iWATs (right panel). Representative images of H&E-stained and UCP1-stained (B) BATs and (C) iWATs. Tissues slides corresponding to successive cuts were used. Scale bars, 100 µm. Data represent means ± SD (n=5 mice/group). Data were analyzed using one-way ANOVA followed by Bonferroni's post hoc test. **p<0.01; ****p<0.0001; ns, not significant.

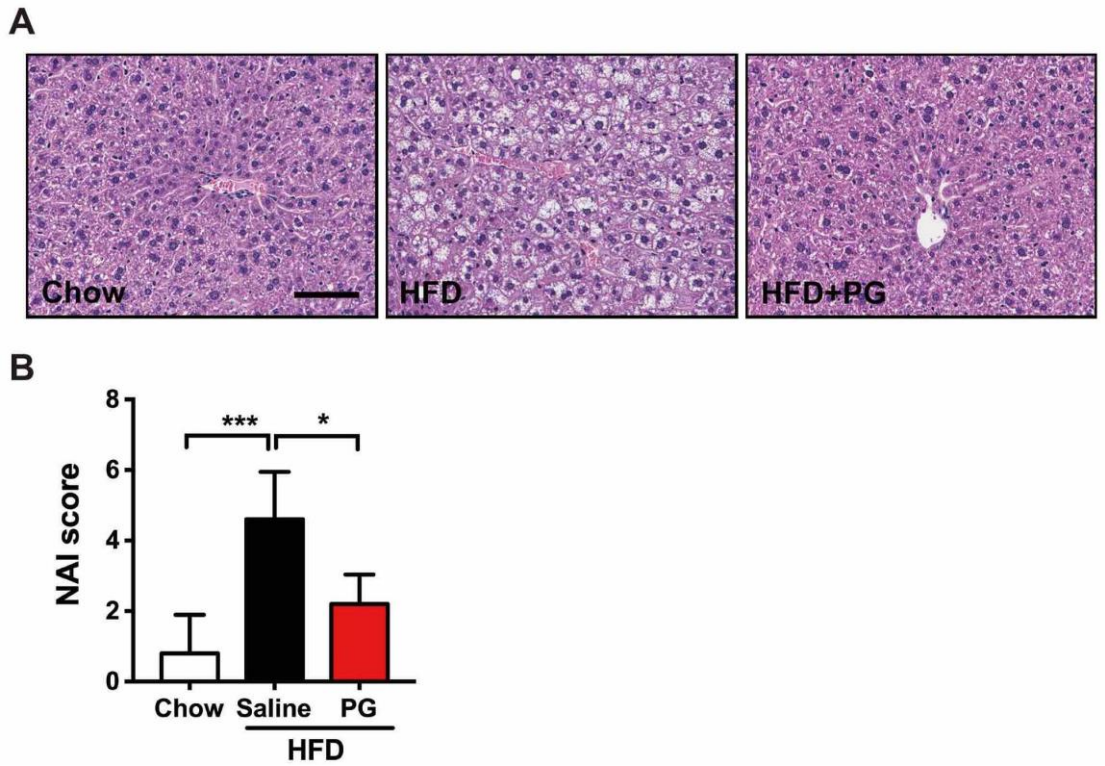

Supplementary figure S22

P. goldsteinii treatment prevents signs of NAFLD and NASH in HFD-fed mice. Experiments were performed as in figure 7. (A) Representative images of H&E-stained liver tissues. Scale bar, 100 µm. (B) NAI score. Data represent means ± SD (n=5 mice/group) and analyzed using one-way ANOVA followed by Bonferroni's post hoc test. *p<0.05; ***p<0.001.

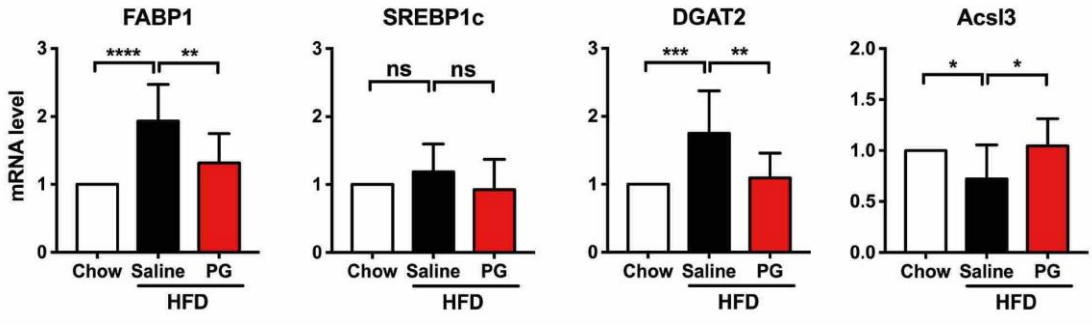

Supplementary figure S23

P. goldsteinii treatment normalizes gene expression involved in lipid metabolism in HFD-fed mice. Experiments were performed as in figure 6. Expression of lipid metabolism genes in the liver, including FABP1, SREBP1c, DGAT2 and Acsl3, was evaluated using qRT-PCR. Data represent means ± SD (n=8 to 11 mice/group). Data were analyzed using one-way ANOVA followed by Bonferroni's post hoc test. *p<0.05; **p<0.01; ***p<0.001; ****p<0.0001; ns, not significant.

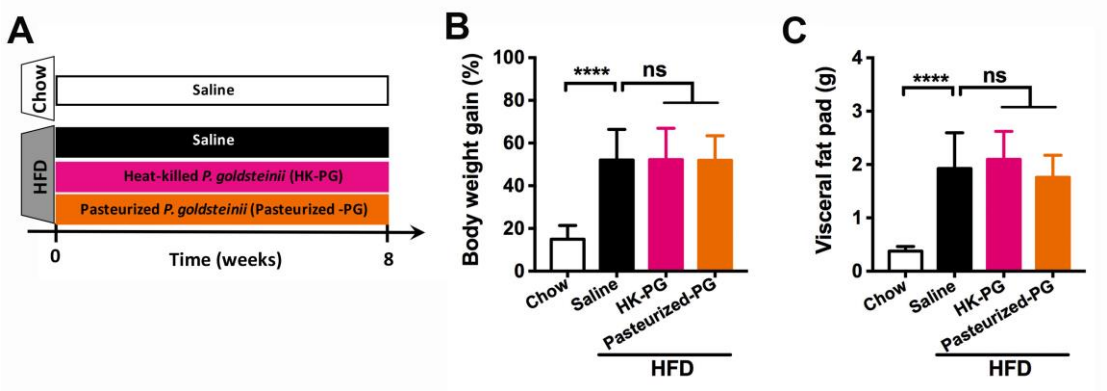

Supplementary figure S24

Heat-killed and pasteurized *P. goldsteinii* fail to prevent obesity in HFD-fed mice. (A) Chow-fed mice and HFD-fed mice were treated daily with saline, heat-killed (HK-PG) or pasteurized *P. goldsteinii* (4×10^7 CFUs each) by oral gavage for 8 weeks. (B) Body weight gain and (C) visceral fat pad weight were monitored after 8 weeks of treatment. Data represent means ± SD (n=10–15 mice/group). Data were analyzed using one-way ANOVA followed by Bonferroni's post hoc test. ****p<0.0001; ns, not significant.

Supplementary table S1

Molecular weight analysis of fractions isolated from HSM water extract

Fraction	Main Compound	Molecular Weight (kDa)	Percentage (%)
H1	Polysaccharides	>300	20.1
H2	Polysaccharides	10–300	30.6
H3	Polysaccharides	<10	7.7
H4	Mono-, di-, oligosaccharides	Undetermined	39.7

Polysaccharides were analyzed from 100 ml of HSM water extract. Shown in the last column are the percentages that each fraction represents based on the total HSM water extract.

Supplementary table S2

Biochemistry analysis of serum of mice treated with *P. goldsteinii* for 8 weeks

Parameters	Chow[a]		HFD	
	Saline	PG	Saline	PG
AST (U/l)	73.89±13.38	76.59±11.19	107.92±31.82*	80.95±17.32[#]
ALT (U/l)	28.66±7.21	26.34±4.98	49.5±30.52*	34.54±13.89
T-BIL (µg/dl)	29.65±6.14	25.12±4.02	43.22±14.38	40.43±13.1
ALB (g/dl)	3.04±0.14	3.09±0.17	2.95±0.19	2.96±0.05
BUN (mg/dl)	32.98±11.79	28.26±2.93	18.4±3.63*	21.88±2.96
CREA (mg/dl)	0.26±0.14	0.21±0.05	0.19±0.05	0.21±0.05
UA (mg/dl)	3.54±2.04	3.28±2.4	2.1±1.83	2.16±1.31

[a]Data represent means ± SD of duplicate experiments (n=6 to 10 mice/group) in mice fed with chow or HFD and orally treated with saline or *P. goldsteinii* (PG; 4×10^7 CFUs).

*Values showing a statistically significant difference ($p<0.05$) compared with the chow-saline group.

[#]Indicates a statistically significant difference ($p<0.05$) compared with the HFD-saline group.

Data were analyzed using one-way ANOVA followed by Bonferroni's post hoc test.

AST, aspartate aminotransferase; ALT, alanine aminotransferase; T-BIL, total bilirubin; ALB, albumin; BUN, blood urea nitrogen; CREA, creatinine; UA, uric acid.

Supplementary table S3

Monosaccharide composition of polysaccharide fraction H1

	Man	Glc	Gal	GlcN	Ara	GalN	Rha	Fuc
Concentration (%)	50.4	12.5	23.8	4.6	1.7	0.4	3.4	3.2

Man, mannose; Glc, glucose; Gal, galactose; GlcN, N-glucosamine; Ara, arabinose; GalN, N-galactosamine; Rha, rhamnose; Fuc, fucose.

Supplementary table S4

PCR primers used in this study

Target	Direction	Primer sequence (5'–3')
Mouse genes		
IL-1β[23]	Forward	TTGAAGAAGAGCCCATCCTC
	Reverse	CAGCTCATATGGGTCCGAC
TNF-α[23]	Forward	TAGCCAGGAGGGAGAACAGA
	Reverse	TTTTCTGGAGGGAGATGTGG
ZO-1[23]	Forward	ACCCGAAACTGATGCTGTGGATAG
	Reverse	AAATGGCCGGGCAGAACTTGTGTA
CD36[24]	Forward	ATGGGCTGTGATCGGAACTG
	Reverse	GTCTTCCCAATAAGCATGTCTCC
Fasn[25]	Forward	GCTGCGGAAACTTCAGGAAAT
	Reverse	AGAGACGTGTCACTCCTGGACTT
HSL[26]	Forward	GCTGGGCTGTCAAGCACTGT
	Reverse	GTAACTGGGTAGGCTGCCAT
LPL[27]	Forward	GGACGGTAACGGGAATGTATG
	Reverse	ACGTTGTCTAGGGGGTACTTAAA
FABP1[28]	Forward	TGGACCCAAAGTGGTCCGCA
	Reverse	AGTTCAGTCACGGACTTTAT
SREBP1c[29]	Forward	GATGTGCGAACTGGACACAG
	Reverse	CATAGGGGGCGTCAAACAG
DGAT2[30]	Forward	ATCTTCTCTGTCACCTGGCT
	Reverse	ACCTTTCTTGGGCGTGTTCC
Acsl3[31]	Forward	GGGACTACAATACCGGCAGA
	Reverse	ATAGCCACCTTCCTCCCAGT
UCP1[32]	Forward	AGGCTTCCAGTACCATTAGGT
	Reverse	CTGAGTGAGGCAAAGCTGATTT
GAPDH[23]	Forward	GCATCCACTGGTGCTGCC
	Reverse	TCATCATACTTGGCAGGTTTC

Human genes		
ZO-1[33]	Forward	GCAGCTAGCCAGTGTACAGTATAC
	Reverse	GCCTCAGAAATCCAGCTTCTCGAA
18S[34]	Forward	GTAACCCGTTGAACCCCATT
	Reverse	CCATCCAATCGGTAGTAGCG
Other genes		
16S rDNA 27F-1492R[35]	Forward	AGAGTTTGATCCTGGCTCAG
	Reverse	GGTTACCTTGTTACGACTT
P. goldsteinii	Forward	GAATAAAGTGAGGAACGTGTT
	Reverse	AACTTTCACCGCTGACTTAATTA
16S rDNA 520R[35] (for cloning sequencing)	Reverse	ACCGCGGCTGCTGGC

Supplementary datasets

Supplementary dataset S1

(Microsoft Excel file). Non-alcoholic steatohepatitis activity index (NAI) assessment.

Supplementary dataset S2

(Microsoft Excel file). Reads generated from next-generation sequencing of each mouse in in vivo antibiotic mouse experiments. Related to figure 4.

Supplementary dataset S3

(Microsoft Excel file). Relative abundance of bacterial species showing differences between the H1-treated group and antibiotics groups after HFD feeding for 12 weeks. Related to figure 4A,B.

Supplementary dataset S4

(Microsoft Excel file). Spearman correlation analysis between the bacterial species identified and obesity traits. Related to figure 4D.

Supplementary dataset S5

(Microsoft Excel file). Relative abundance of bacterial species showing differences between the H1-treated donor group and antibiotics donor groups after HFD feeding for 12 weeks. Related to figure 6A,B.

Supplementary dataset S6

(Microsoft Excel file). Relative abundance of bacterial species showing differences between the H1-treated recipient group and antibiotics recipient groups after HFD feeding for 12 weeks. Related to figure 6C,D.